Table1.HrHPV results one year prior histological diagnoses of cervical cancers.

Types	Cases	HPV positive(%)	HPV negative(%)
SCC	332	316(95.2)	16(4.8)
ADC	45	34(75.6)	11(24.4)
Total	377	350(92.8)	27(7.2)

1271 Probable Causes of Recurrent Low-Grade Endometrioid Cancers

Wenxin Zheng, Yiying Wang, Yue Wang, Zhenbo Zhang, Hong Liao. University of Arizona College of Medicine, Tucson, AZ; Henan Provincial People's Hospital, Zhengzhou, Henan, China.

Background: Endometrial carcinoma is the most common gynecologic malignancy and has two major histological types, endometrial endometrioid carcinoma (EEC) and endometrial serous carcinoma (ESC). EECs typically have a much better prognosis than those ESCs. However, there are approximately 10% of patients with low-grade EECs who recur within a few years after total hysterectomy and staging. Such patients have a poor clinical course. It is currently unclear what causes the tumor recurrence.

Design: We have collected a total of 40 EEC patients who had tumor recurrence in less than 4 years after surgery. These included 30 FIGO grade 1 and 10 FIGO grade 2 EECs. Clinicopathologic data were recorded. All cases were histologically reviewed and the representative tumor sections were subsequently examined by immunohistochemistry [(p53, IMP3, and MMR protein (MLH1, PMS2. MSH2, MSH6)] and by PCR analysis for K-ras (codons 12 and 13) gene.

Results: BMI of the patients ranged from 21 to 27 with an average of 23.5. Patients' age ranged from 35 to 76 with average of 55.6 years. Among the 40 recurrent EEC cases, 6 (15%) were ESC (confirmed with p53 and IMP3 staining), 8 (20%) were Lynch syndrome associated endometrial cancer (confirmed with MMR protein staining and subsequent DNA sequence analysis), 5 (12.5%) were positive for IMP3, and 7 (17.5%) had K-ras mutation in either codon 12 or 13. Interestingly, among the 7 EEC cases with K-ras mutation, 6 of them showed significant (>30% of total tumor volume) mucinous differentiation. It is unclear what the genetic alterations are for the remaining 14 (35%) cases.

Conclusions: The majority recurrent cases may be caused by genetic alterations of TP53, IMP3, K-ras or Lynch syndrome associated DNA repair genes. It is necessary to evaluate apparently "low-grade" endometrioid carcinoma carefully to rule out serous or mucinous endometrial cancer. This is particularly true for those patients without clinical evidence of estrogen overstimulation or without endometrial hyperplasia in the background. Correct identifying such cancer patients before or after definitive surgery will have a significant clinical impact for patient care.

1272 p16 INK4a/ProExC/Mib-1 Have Similar Expression Patterns in Both HPV 16/18 and Non-16/18 High Risk HPV Positive Cervical Dysplasia and Help With the Diagnosis of Deceiving Dysplasia

Haijun Zhou, Michael Deavers, Kristi Perez, Dina Mody, Yimin Ge. Houston Methodist Hospital, Houston, TX.

Background: HPV infection is a well-known causative agent for the vast majority of cervical dysplasias and cancers in women. The HPV genotype-specific histologic features and expression patterns of $p16^{INK4a}$, ProExC and Mib-1 in cervical squamous dysplasia are not fully studied.

Design: From 1/2010 to 4/2011, 808 SurePath cervical specimens from the dysplasia clinic were collected and tested for 40 HPV genotypes by DNA microarray. Immunohistochemical stains for $p16^{INK4a}$/ProExC/Mib-1 were performed on 115 biopsies sampled within 6 months of the Pap tests. The expression patterns (p16: block positive, patchy positive and negative; ProExC and Mib-1: basal positive (1+), lower 1/3 positive (2+) and more than lower 1/3 positive (3+)) and intensity scores (percentage of positive cells in epithelium) were recorded. The histologic patterns were classified into conventional dysplasia and deceiving dysplasia that was characterized by atypical squamous cells with enlarged nuclei and increased N/C ratios, vesicular chromatin, lack of hyperchromasia, and few mitotic figures. Correlation of histology, immunohistochemistry and HPV genotypes was performed.

Results: All 115 cases had dysplastic changes with 52 cases of CIN2+. Dysplasia cases with HPV 16/18 had 62.5% with p16 block positivity, 65.0% with ProExC 3+ positivity (intensity score 30-100%) and 62.5% with Mib-1 3+ positivity (intensity score 20-95%), respectively. Dysplasia cases with non-16/18 high risk HPV (HR-HPV) infection had 55.1% with p16 block positivity, 40.8% with ProExC 3+ positivity (intensity score 30-95%) and 61.2% with Mib-1 3+ positivity (intensity score 5-95%), respectively. Strikingly, only 3 of 21 cases with deceiving dysplasia (14.3%) had conventional CIN2+ lesions, while p16/ProExC/Mib-1showed block and/or 3+ positivity in 18 cases (85.7%) (14 cases with p16 block positive, 4 cases with Mib-1 3+ positive and 2 cases with both ProExC and Mib-1 3+ positive). Interestingly, the majority of the deceiving dysplasia cases were infected by non-16/18 HR-HPV (n=14, 66.7%) with only a few by HPV 16/18 (n=2, 9.5%).

Conclusions: The expression patterns of p16/ProExC/Mib-1 do not differentiate cervical dysplasia caused by HPV 16/18 from those caused by non-16/18 HR-HPV genotypes (p=0.73/0.2/1.0). However, p16/ProExC/Mib-1 can significantly aid in the detection of deceiving dysplasia compared to H&E stain alone ($p<0.001$), and deceiving dysplasia was more commonly positive for non-16/18 HR-HPV in this cohort.

Head and Neck Pathology

1273 SMARCB1(INI1)-Deficient Sinonasal Carcinomas: Expanding the Morphological Spectrum of a Recently Described Entity

Abbas Agaimy, Helene Geddert, Bruno Markl, Marc-Oliver Riener, Wilko Weichert, Arndt Hartmann. University Hospital of Erlangen, Erlangen, Bavaria, Germany; St. Vincent's Hospital, Karlsruhe, Germany; Klinikum Augsburg, Augsburg, Germany; University Hospital of Heidelberg, Heidelberg, Germany.

Background: Recently, a variant of sinonasal tract carcinoma characterized by complete loss of nuclear SMARCB1 (INI1) has been described. A majority of reported cases (total: 13) showed a predominantly undifferentiated basaloid "blue" appearance.

Design: To define its clinicopathological spectrum, we identified 8 additional cases of this rare entity from our files and from four other collaborative institutions, in addition to our previously reported three original cases (total: 11 patients). We performed immunohistochemistry, HPV genetic testing and fluorescence in situ hybridization (FISH) studies.

Results: Patients were 9 women and 2 men (aged 28-76; mean, 46). All presented with advanced local disease (pT4). No family history of rhabdoid tumors or history of prior exposure to radiation was known. Surgery (radical or partial resection) and adjuvant or palliative chemo-/radiation was the treatment in all cases. All but one of 7 patients with detailed follow-up developed metastases and 2 died of disease at 22 and 102 months, respectively. Histological examination showed a predominance of basaloid (7), eosinophilic/rhabdoid (2), oncocytoid (1) and squamoid (1) cell features. Diffuse or partial p16 expression was observed in most of cases but none contained high risk HPV DNA. Immunohistochemistry showed strong expression of pancytokeratin with variable expression of CK5, p63, vimentin and focal reactivity for neuroendocrine markers. All cases showed complete loss of nuclear SMARCB1 expression by immunohistochemistry. SMARCB1 FISH analysis was successful in 5 cases: 1 showed biallelic deletion, and two cases each showed monoallelic deletion and intact SMARCB1.

Conclusions: SMARCB1-deficient carcinomas of sinonasal tract represent a distinctive emerging entity among poorly differentiated/ undifferentiated sinonasal carcinomas with predilection for middle-aged women, variable heterogeneous (mainly basaloid) morphology and variably aggressive clinical course. Their molecular pathogenesis seems to be heterogeneous as well. While some cases show biallelic SMARCB1 deletions, others feature monoallelic alterations or even lack SMARCB1 alterations by FISH suggesting other yet unidentified molecular mechanisms responsible for the SMARCB1 loss.

1274 Telomere Shortening in Oral Epithelium in Relation To ADH-1B and ALDH-2 Genotypes and Clinicopathologic Findings

Junko Aida, Akira Yokoyama, Naotaka Shimomura, Ken-ichi Nakamura, Naoshi Ishikawa, Mutsunori Fujiwara, Yoko Matsuda, Tomio Arai, Kaiyo Takubo. Tokyo Metropolitan Institute of Gerontology, Tokyo, Japan; National Hospital Organization Kurihama Alcoholism Center, Yokosuka, Japan; Japanese Red Cross Medical Center, Tokyo, Japan; Tokyo Metropolitan Geriatric Hospital, Tokyo, Japan.

Background: Telomeres are repetitive G-rich DNA sequences and associated binding proteins found at the ends of eukaryotic chromosomes, and appear to play a key role in preventing genomic instability. Progressive telomere shortening with age or chronic inflammation may lead to genomic instability that characterizes the early stage of carcinogenesis. Certain risk factors, such as drinking alcoholic beverages, smoking, or papilloma viral infection, predispose the oral mucosa to squamous cell carcinoma. It is known that the ALDH-2 and ADH-1B genotypes influence the risk of cancer due to alcohol drinking. In the esophagus, iodine-unstained areas and their multiplicity revealed by chromoendoscopy are known to be related to telomere shortening. In the present study, we analyzed telomere lengths in the oral mucosa in relation to cancer risk factors.

Design: All tissues were examined histopathologically. Using our Q-FISH technique, we estimated telomere lengths of epithelial basal cells in the background mucosa from 23 cases of mucosal carcinoma, 12 cases of dysplasia, and 22 non-neoplastic cases. ALDH2 and ADH1B genotypes were determined using DNA extracted from paraffin sections. We analyzed telomere lengths in relation to drinking, smoking, p16 immunoreactivity, and cancer multiplicity.

Results: Telomeres in the backgrounds of dysplasia and mucosal carcinoma were significantly shorter than in controls. In the ADH1B less active type (*ADH1B*1/*1*) they were shorter than in the adult control group ($p = 0.038$), but not significantly shorter in the ALDH2 inactive type (*ALDH*1/*2 or *2/*2*) ($p = 0.841$). Drinkers and patients with multiple oral cancers tended to have shorter telomeres, but not to a significant degree. There was no significant correlation of telomere length with smoking index or p16 positivity.

Conclusions: Telomeres in the oral epithelium are shorter in cases of oral dysplasia or mucosal carcinoma than in non-neoplastic controls. In addition, telomeres are shorter in the ADH1B less active group than in the active group, despite the lack of any evident difference in the esophageal epithelium of alcoholics. Telomeres in the oral epithelium may be directly affected by alcohol drinking.

1275 Early pT1 Oral Squamous Cell Carcinomas Identified in the Setting of an Oral Dysplasia Clinic Commonly Exhibit Adverse Histologic Prognostic Features

Maimuna Al Saadi, Esther O'Regan, Mary Toner. St. James Hospital, Dublin, Ireland; Dublin Dental University Hospital, Dublin, Ireland.

Background: Much of the literature on prognostic histopathologic features on oral squamous cell carcinomas(OSCC) excludes early OSCC and decisions about further surgical management of these cases may be problematic. Since the advent of a multidisciplinary oral dysplasia clinic, we have encountered increasing numbers of early OSCC, sometimes within an excision biopsy of a white lesion.

Design: _All pT1 OSCC from 2009-2013 were reviewed for tumour maximum dimension, depth, perineural invasion (PNI), lymphovascular invasion (LVI), worst pattern of invasion (WPOI) score 4 or 5, and nodal status, to document how frequently OSCC that were small (size 10mm or less, group A) and thin (depth of 4mm or less, group B) exhibit recognised adverse pathologic features and node positivity. WPOI 4 indicates an invasive tumour front with small tumour islands of 15 cells or fewer; WPOI 5 indicates tumour satellites 1mm or more from main tumour (Brandwein-Gensler M *et al* Am J Surg Pathol 2005:29;167-178).

Results: Out of 103 pT1 tumours, there were 51(49%) small OSCC (group A) and 74(72%) thin OSCC (group B).

Of the 51 small OSCC, 7(14%) had a depth of >4mm, 5(10%) showed PNI, 2(4%) showed LVI, 28(56%) showed WPOI 4 and 5(6%) showed WPOI 5. 29(39%) had a depth of 5mm or more and 7(9 %) had a depth of 8mm or more. 5(10%) were node positive, stage pN1(3), stage pN2(2).

In 74 thin OSCC, PNI and LVI was rare, but WPOI 4 or 5 was seen in 43(58%). 9% of thin OSCC were node positive, stage pN1(1), stage pN2(6). Two node positive tumours were 2mm or less in depth.

Of the 43 OSCC that were both small and thin, 3(6%) showed PNI, none showed LVI, 25(58%) showed WPOI 4 and 1 showed WPOI 5 and 2(4%) were node positive, all of which were stage pN2. Despite the potential for difficulty in assessing WPOI at a biopsy site in a thin OSCC, this was only a problem in 2/103 cases.

Conclusions: Small OSCC commonly exhibit adverse pathologic features including WPOI 4 or 5 in >60%, a depth of 5mm or more in 39% and node positivity in 10%. 58% of thin carcinomas showed WPOI 4 or 5, and 9% were node positive. In addition, 6% of tumours that were both small and thin were stage pN2.

1276 A Quantitative Histomorphometric Classifier Identifies Role of Stromal and Epithelial Features in Prediction of Disease Recurrence in p16+ Oropharyngeal Squamous Cell Carcinoma

Sahirzeeshan Ali, James Lewis, Anant Madabhushi. Case Western Reserve University, Cleveland, OH; Washington University, St. Louis, MO.

Background: Human papillomavirus-related (p16 positive) oropharyngeal squamous cell carcinoma (OSCC) represents a steadily increasing proportion of head and neck cancers and has a favorable prognosis. However, approximately 10% of patients develop recurrent disease. Quantitative measurements (via construction of graphs with nuclei as vertices) of spatial arrangement of nuclei in histopathology images for different cancers have been shown to have prognostic value. There has been recent interest in looking at possible role of interactions between stromal and epithelial regions in disease aggressiveness. We sought to develop an image-based predictor to identify new features in OSCC by quantitative characterization of spatial interactions within stroma and epithelial regions, thereby providing new insights into the biological factors driving the progression of OSCC disease.

Design: Using a tissue microarray cohort of p16 positive OSCC cases (scanned H&E images) with clinical follow up, were marked binarily according to tumor recurrence versus none. Each nucleus was identified via an automated computerized image analysis algorithm. Then, using a novel cell graph that allowed for implicit construction of two separate nuclear graph within each of the stromal and epithelial regions, we were able to explore the combined contribution of stroma and epithelium by measuring the spatial distribution and clustering of cells, a series of topological features defined on each node of the subgraph in both compartments. A random forest classifier was developed, independently trained and validated over 10 runs of 3-fold cross validation.

Results: There were 160 p16+ patients on the array, of whom 19 developed recurrent disease. The classifier was correct in 145 cases (**90.6%**) (Table 1).

	Only Epithelial	Only Stroma	Using Both Regions
Accuracy	86.2±1.2	68.1±0.2	90.6±1.5
PPV(P)	85.2±1.6	76.1±0.2	89.4±0.2
PPV(NP)	82.5±2.6	78.7±0.2	86.5±0.5

Conclusions: Based only on tiny H&E punches, a computer-aided morphometric classifier analyzing stromal and epithelial compartments can strongly predict tumors at low likelihood of recurrence and suggest those at higher risk. With further validation, this may be a very useful in practice to select patients for de-escalated therapies versus those who should receive more aggressive treatment.

1277 Performance of a Branch Chain RNA In-Situ Hybridization Assay for the Detection of High-Risk Human Papillomavirus in Head and Neck Squamous Cell Carcinoma

Kshitij Arora, Darcy Kerr, Krishnan Mahadevan, Jason Hornick, Jeffrey Krane, Miguel Rivera, David Ting, Vania Nose, Peter Sadow, Vikram Deshpande, William Faquin. Massachusetts General Hospital, Boston, MA; Brigham & Women's Hospital, Boston, MA.

Background: High-risk human papillomavirus (hr-HPV) infection is a major etiologic agent in a subset of head and neck squamous cell carcinomas (HNSCCs), and its recognition has prognostic and predictive implications. There is no single robust test to assess hr-HPV status. The objective of this study is to assess a branch chain RNA *in-situ* hybridization (ISH) assay for detecting hr-HPV in HNSCC and to compare these results with conventional hr-HPV specific tests (DNA ISH and PCR) and the hr-HPV surrogate marker, immunohistochemistry for p16.

Design: We reviewed clinicopathologic details and ancillary testing results for 37 patients with HNSCC. All cases were also stained with an RNA ISH assay (QuantiGene®ViewRNA technology (Affymetrix, Santa Clara, CA)), which recognizes 12 hr-HPV types (types 16, 18, 31, 33, 35, 39, 45, 51, 52, 56, 58 and 66).

Results: RNA ISH was technically successful in 35/37 cases (95%). Of these, RNA ISH was positive in all cases positive for hr-HPV by DNA ISH (n=14) and PCR (n=9). Most cases positive for p16 were also positive by RNA ISH (90%).

Table 1: Successful RNA ISH cases

		RNA ISH Positive (n=29)	RNA ISH Negative (n=6)
DNA ISH (n=25)	+	14 (56%)	0 (0%)
	-	11 (44%)	6 (100%)
PCR (n=13)	+	9 (69%)	0 (0%)
	-	4 (31%)	6 (100%)
p16 (n=29)	+	26 (90%)	1 (17%)
	-	3 (10%)	5 (83%)

Nine cases positive by RNA ISH did not have another specific hr-HPV test available that corroborated the presence of hr-HPV. The majority (n=6/9) were positive for p16, but 4 were negative for hr-HPV by PCR and 7 were negative by DNA ISH.

Table 2: RNA ISH+ cases without other specific hr-HPV marker

Case	PCR	DNA ISH	p16
1	-	Inconclusive	+
2	-	-	-
3	-	-	-
4	-	-	-
5		-	+
6		-	+
7		-	+
8		-	+
9			+

All cases that were negative for hr-HPV by RNA ISH (n=6) were also negative by DNA ISH and PCR.

Conclusions: Branch chain RNA ISH confers great sensitivity in detecting hr-HPV in HNSCC, recognizing all cases classified as positive for hr-HPV by DNA ISH and PCR. RNA ISH also detects additional cases that may not be identified by the other hr-HPV specific methods. Analysis of a larger cohort and correlation with patient outcome is warranted to determine whether this assay reflects a desirable level of clinical specificity for hr-HPV associated HNSCC.

1278 Primary Tumors of the External Auditory Canal: Experience of 194 Cases at a Single Tertiary Care Oncology Centre

Munita Bal, Asawari Patil, Shubhada Kane, Rajiv Kaushal, Pankaj Chaturvedi, Jai Agarwal, Anil D'Cruz. Tata Memorial Hospital, Mumbai, Maharashtra, India.

Background: Primary neoplasms of external auditory canal (EAC) are rare tumors. Our aim was to study the clinicopathologic spectrum of EAC tumors diagnosed at our centre.

Design: A retrospective review of clinical and pathologic data of EAC tumors diagnosed from 2003-2013 was undertaken.

Results: 194 EAC tumors were included. Median age was 55yrs (6–88yrs). Ear discharge >10 yrs & facial nerve involvement was seen in 36% & 21%, respectively. Post-radiation sarcomatoid carcinoma was seen in 2; 1 sebaceous carcinoma was part of Muir-Torres syndrome.

CARCINOMA	168	SARCOMA	10
Squamous	135	Rhabdomyosarcoma, embryonal	6
Adenoid cystic	13	Leiomyosarcoma	1
Ceruminous	4	Malignant peripheral nerve sheath tumor	1
Sebaceous	4	Osteosarcoma	1
Sarcomatoid	3	Giant cell tumor	1
Basaloid	3	HEMATOLYMPHOID MALIGNANCY	6
Trichilemmal	2	Langerhans cell histiocytosis	3
Transitional	1	Diffuse large B-cell lymphoma	1
Lymphoepithelial	1	Multiple myeloma	1
Small cell	1	Granulocytic sarcoma	1
Basal cell	1	MALIGNANT MELANOMA	4
		JUGULOTYMPANIC PARAGANGLIOMA	3
HEMANGIOMA	1	SCHWANNOMA	2

Table1: Pathologicspectrum of EAC neoplasms

98 malignant cases underwent radical resection. Tumor size ranged from 0.5-8 cm (mean 2.8 cm). T stages: T1-12%, T2-16%, T3-42% and T4-30%. Rate of parotid involvement was 9%. Rate of resection margin involvement was 36%; commonest involved was medial margin; R1 rate correlated with higher T stage. Nodal metastasis was seen in 22% cases; commonest site was level II node. 57 patients received adjuvant therapy. Follow-up ranged from 3-119 months (median, 26 months); 22 patients developed local recurrence (median time-to-recurrence, 20 months); 13 patients developed distant metastasis; common sites included lung, liver and bone.

Conclusions: Squamous cell carcinoma is the commonest malignancy of EAC. However, diverse pathologic entities may uncommonly present as neoplasms of EAC. Accurate diagnosis employing immunohistochemistry when required is essential for the optimal management of these rare tumors. Early diagnosis and treatment might offer a chance of complete excision and better outcome.

1279 Lymphatic Endothelial Mimicry (or Lymphatic Endothelial Cancerization) in Papillary Thyroid Carcinoma: Hidden Evidence of Lymphatic Invasion and Histopathogenesis of Cystic Metastasis in Cervical Lymph Nodes

Christopher Ball, Luan Truong, Chi Lai, Bibianna Purgina, Kien Mai. University of Ottawa, Ottawa, ON, Canada.

Background: We hypothesize that cystic structures in metastatic papillary thyroid carcinoma (PTC) develop along the framework of lymphatic channels.

Design: To investigate this phenomenon of lymphatic endothelial cancerization or lymphatic endothelial mimicry in PTC, different types of PTC were immunostained for D2-40 and TTF1.

Results: Thirty cases of PTC with lymph node metastasis or with potential for lymphatic invasion, and 20 cases of metastatic PTC in lymph nodes were reviewed; 40-100 % of cases showed double/mosaic immunoreactivity for TTF1/D2-40. Lymph nodes with PTC metastasis, cysts, and branching cleft-like spaces lined by follicular cells with or without nuclear features of PTC were diffusely reactive to TTF1 and focally reactive to D2-40. In addition, for solid and cystic primary and metastatic PTC, extensive TTF1 reactivity and focal or extensive D2-40 reactivity were also demonstrated in cystic or cleft linings. For 25 thyroid neoplasms with no known potential for lymphatic invasion, there was no such immunoreactivity.

Conclusions: Evidence of endothelial mimcry of follicular thyroid cells or lymphatic endothelial cancerization is supported by the double or mosaic immunoreactivity for TTF1/D2-40. Double/mosaic immunoreactivity is highly specific in identifying PTC with lymphatic invasion in primary thyroid lesions. Positive D2-40 immunoreactivity in follicular cells suggests that a) most metastatic cystic PTCs represent lymphatic endothelial cancerization, and b) there is hidden evidence of lymphatic invasion in primary thyroid tumors with potential for lymph node metastasis.

1280 Translocation and Expression of MSANTD3 in Neoplasia and Normal Tissue

Nicholas Barasch, Gong Xue, Robert Sweeney, Sushama Varma, Jewison Biscocho, Kevin Kwei, Robert Pelham, Joseph Lipsick, Robert West, Jonathan Pollack. Stanford University School of Medicine, Stanford, CA.

Background: Recurrent fusion genes have been identified in multiple different salivary tumors; however, a recurrent translocation has not yet been identified in Acinic Cell Carcinoma (AcCC). Recent advances in transcriptome sequencing (RNAseq) provide a new opportunity to find driving mutations.

Design: We utilized RNAseq on three archival cases of AcCC to identify novel translocations. Based on these findings, we performed targeted fluorescence in situ hybridization (FISH) and immunohistochemical (IHC) analysis on microarrays of 27 individual archival AcCC cores to determine if a translocation was recurrent and if the translocation resulted in gene over-expression. We next determined the AcCC specificity of a translocation and gene expression by performing FISH and IHC on microarrays containing 220 other individual neoplastic and benign salivary gland cores and IHC on 1075 benign and neoplastic cores from the gastrointestinal, neural, endocrine, genitourinary, and cardiorespiratory systems, breast and the head and neck region.

Results: Using RNAseq, we identified a translocation between the gene Myb/SANT-Like DNA-Binding Domain Containing protein 3 (MSANTD3/C9orf30/L8) and Histatin 3 (HTN3) t(9;4)(q31-32;q13-14) in one of three cases of AcCC. The predicted product is consistent with the HTN3 promoter driving overexpression of the full-length MSANTD3 gene. MSANTD3 shares homology with MYB, which has been demonstrated to be a neoplastic driver in a recurrent translocation of salivary adenoid cystic carcinoma (ACC). Using our microarray, we found this MSANTD3 break-apart to be recurrent in 15% (4/27) of AcCC by FISH. IHC staining for MSANTD3 demonstrated diffuse nuclear protein expression in 30% (8/27) of AcCC. The four FISH break-apart specimens were amongst these eight. MSANTD3 IHC staining of the salivary cores showed acinar cells of normal salivary tissue are nearly always negative for MSANTD3 while ductal cells express the protein variably. A subset of salivary neoplasms, including 20% of mucoepidermoid carcinomas, also express MSANTD3 without an MSANTD3 break-apart by FISH. Strong IHC expression was also seen in spermatogonia, renal tubular cells, gastric parietal cells, adrenal cortex, prostatic glands and endometrium and in specific cancers of the testicle, liver, bladder, stomach, lung, prostate and breast.

Conclusions: Our findings show that an MSANTD3 break-apart is present in 15% of AcCC and may be a novel oncogenic driver of this salivary tumor. Furthermore, we also find that MSANTD3's expression in other varied carcinomas may possibly suggest a wider role of this gene in cancer.

1281 Next-Generation Sequencing Reveals Rare Genomic Alterations in Sinonasal High-Grade Carcinomas FFPE Samples

Diana Bell, Rajesh Singh, Russell Broaddus, Randal Weber, Ehab Hanna. University of Texas MD Anderson Cancer Center, Houston, TX.

Background: Malignant sinonasal tumors can present with an undifferentiated or poorly differentiated morphology (e.g. esthesioneuroblastomas, sinonasal undifferentiated carcinoma and neuroendocrine carcinomas). We witnessed advances in diagnosis and therapeutic modalities leading to improvements in survival, however, the optimal treatment for these remain debated.

Genotyping is increasingly performed in tumor types where mutational status may drive treatment choice. Next-generation sequencing can expand on genotyping of individual base pairs ; it can detect mutations across entire exons, copy changes and fusion genes. For NGS to be clinically viable, it must be made compatible with FFPE tissues and concordant with best current diagnostic methods.

Design: We selected 10 FFPE specimens of primary sinonasal tumors. Genotyping and sequencing were both performed in CLIA compliant labs.

Results: The included histologies were as follow: 5 sinonasal undifferentiated carcinomas (SNUC), 2 high-grade neuroendocrine carcinomas, small cell type (HG-NEC), 2 low-grade esthesioneuroblastomas (ENB Hyams grade 2/4) and one high-grade esthesioneuroblastoma (ENB Hyams grade 4/4).

We identified several mutated genes/ somatic mutations and copy number variations. Mutations were identified in known cancer genes, (*MAGEA1, PKHD1, EP400 and TRRAP).* Mutations in *MAGEA1* (exon 3) was identified in 1 SNUC; 3 SNUCs showed no genomic alteration and one SNUC did not amplify. One HG-NEC showed *PKHD1* (exon 13) mutation amplification of NFE2L2. Loss of CIC was detected in the high-grade ENB, while the other 2 low-grade ENB had *EP400* (exon 8) and *TRRAP*(exon 49) somatic mutations along with 6 polymorphisms.

Conclusions: In contemporary oncology practices there is an increasing emphasis on concurrent evaluation of multiple genomic alterations within the biological pathways driving tumorigenesis.

Our results demonstrate technical feasibility and highlight potential benefits of comprehensive cancer gene characterization through next-generation sequencing of clinical FFPE specimens. As NGS is the most practical means to detect all classes of somatic alteration in a small, clinically relevant sample, we suggest that this type of testing will become an essential component of patient care.

Given the limited treatment options and poor prognosis of patients with high-grade sinonasal carcinoma, comprehensive genomic profiling has the potential to identify new treatment paradigms and meet an unmet clinical need for these diseases.

1282 MYB Translocation Status in Classic and Variant Forms of Salivary Epithelial-Myoepithelial Carcinoma

Justin Bishop, William Westra. Johns Hopkins Hospital, Baltimore, MD.

Background: Epithelial-myoepithelial carcinoma (EMC) is a malignant salivary gland neoplasm defined by tightly coupled biphasic populations of ductal and myoepithelial cells. Classic EMC is well circumscribed, cytologically bland, and regarded as low-grade. Some examples of EMC, however, demonstrate higher grade features with increased cytologic atypia and infiltrative growth. EMC, particularly the higher grade forms, exhibits considerable morphologic overlap with adenoid cystic carcinoma (ACC) - another salivary tumor comprised of ductal and myoepithelial cells. In fact, hybrid carcinomas showing features of both tumors are well described. Up to 50% of ACCs harbor MYB-NFIB gene rearrangements which are believed to be specific for ACC. However, only a handful of EMCs have been tested for the translocation. We sought to clarify the relationship between EMC and ACC by determining MYB translocation status in both classic and variants forms of EMC.

Design: The surgical pathology archives of The Johns Hopkins Hospital was searched for cases of EMC, and 29 cases were retrieved. These included 15 classic low-grade EMCs in addition to 14 variants: 8 intermediate-grade EMCs, 3 hybrid EMC-ACCs, 2 EMCs with myoepithelial atypia, and 1 EMC with high grade transformation (HGT). All cases met histologic criteria for EMC as established by the WHO Classification for Tumors of the Head and Neck. Break apart FISH was performed on all cases. For the hybrid EMC-ACCs and the EMC with HGT, both tumor components were analyzed.

Results: Six of 29 (21%) EMCs were positive for MYB rearrangement by FISH. The positive cases included 3 of 3 (100%) hybrid EMC-ACCs, 2 of 8 (25%) intermediate

grade EMCs, and 1 of 1 (100%) EMCs with HGT. For the hybrid EMC-ACCs and EMC with HGT, both components harbored the rearrangement. In contrast, all cases of classic EMC (0 of 15) and EMC with myoepithelial atypia (0 of 2) were negative for MYB rearrangement.

Conclusions: A subset of tumors meeting diagnostic criteria for EMC harbor MYB rearrangement, an alteration previously thought to be specific for ACC. The fact that MYB rearrangements were limited to intermediate grade EMCs and hybrid EMC-ACCs suggests that either these unusual EMCs are closely related to ACC or that they are, in fact, ACC masquerading as EMC. On the other hand, finding that classic, low grade EMC consistently lacks MYB translocation confirms that, despite morphologic similarities, it is molecularly distinct from ACC. The diagnostic criteria for EMC may need to be refined to underscore the distinction between classic EMC and more ACC-like forms.

1283 High Prevalence of Somatic EGFR Mutations in Inverted Sinonasal Papillomas and Associated Sinonasal Squamous Cell Carcinomas

Noah Brown, Aaron Udager, Jonathan McHugh, Bryan Betz, Megan Lim, Kojo Elenitoba-Johnson. University of Michigan, Ann Arbor, MI.

Background: Sinonasal (Schneiderian) papillomas are clonal proliferations of sinonasal epithelium and are classified into three histologic subtypes – inverted, exophytic, and oncocytic. Inverted sinonasal papillomas (ISP) account for 70% of all sinonasal papillomas and usually arise from the lateral wall of the nasal cavity, from which they can extend along the sinonasal epithelium to involve the ethmoid, maxillary, frontal, and sphenoid sinuses. Approximately 10-15% of cases are associated with a synchronous or metachronous squamous cell carcinoma (SCC). No pathogenic mutations have been reported in ISP or associated SCC, nor has the putative role of ISP as a precursor to SCC ever been demonstrated at the molecular level.

Design: To discover ISP-associated mutations, we screened 8 cases using the Ion AmpliSeq Cancer Hotspot Panel. Somatic mutations were confirmed using bidirectional Sanger sequencing of tumor and matched constitutional DNA. An expanded cohort of cases, including an additional 19 ISP, 8 ISP-associated SCC, 9 exophytic sinonasal papillomas, and 2 oncocytic sinonasal papillomas, was evaluated by targeted Sanger sequencing of *EGFR* exons 18, 19, 20, and 21.

Results: Mutations in epithelial growth factor receptor *(EGFR)* were identified all eight ISPs initially screened by next generation sequencing and 21 of 27 (78%) of all cases evaluated. 7 of 8 (88%) ISP-associated squamous cell carcinomas also demonstrated *EGFR* mutations with identical mutations in all 6 cases with available matched DNA from ISP and the associated SCC. All mutations identified were insertions or deletion/insertions in exon 20 except for one ISP with a missence mutation in exon 19. While a wide variety of length-affecting mutations were identified, several have previously been described in lung adenocarcinoma and have been shown to result in constitutive activation. No *EGFR* mutations were identified in exons 18-21 of either oncocytic or exophytic sinonasal papilloma.

Conclusions: This is the first report of high-frequency, somatic *EGFR* mutations in ISP and ISP-associated SCC. The presence of identical mutations in ISP and associated SCC supports the putative role of ISP as precursor for a subset of sinonasal SCC. The identification of *EGFR* mutations also represents an important development in our understanding of the pathogenesis of ISP and sinonasal SCC and may have significant implications for diagnosis and targeted therapy.

1284 Perineural Invasion (PNI) as a Risk Factor for Local Recurrence (LR) in Early Squamous Cell Carcinoma of the Oral Tongue

Aurelia Busca, Simion Chiosea, Raja Seethala, Lester Thompson, Margaret Brandwein-Gensler, Chi Lai, Susan Robertson, Jessica Maxwell, Uma Duvvuri, Seungwon Kim, Jonas Johnson, Robert Ferris, Esmeralda Marginean, Bibianna Purgina. University of Ottawa, Ottawa, ON, Canada; University of Pittsburgh Medical Center, Pittsburgh, PA; Southern California Permanente Medical Group, Woodland Hills, CA; The University of Alabama at Birmingham, Birmingham, AL.

Background: The significance of PNI as a predictor of LR or as an indication for post-operative radiotherapy (PORT) remains controversial in early oral tongue squamous cell carcinoma (OTSCC). However, the histologic characteristics of PNI in OTSCC are rarely considered. The purpose of this study is to evaluate the prognostic utility of histological patterns of PNI.

Design: Patients with pT1-2, pN0 OTSCC were retrospectively identified in four institutions. PNI was assessed according to nerve size, number of foci, and location subgroups (intratumoral PNI (IT), peripheral PNI (P), and extratumoral PNI (ET)). These subgroups were merged into groups A = P or ET and B = no PNI or IT. Kaplan Meier survival analysis was conducted to compare the time (months) to LR.

Results: Of 256 cases, 81 (31.6%) showed PNI. All but one PNI foci were ≤ 1 mm. Irrespective of PORT, the presence or absence of PNI or the number of PNI foci did not correlate with time to LR. Patients with IT behaved similarly to those without PNI. Kaplan Meier survival analysis showed that for the PNI location groups A (n=57) and B (n=199), median times to LR were 35.00±5.12 (A) and 65.00±9.66 (B) and the log rank test showed statistically significant difference among the survival distributions, $c^2(1)=14.82$, $p<0.001$. Groups A and B were then analyzed controlling for PORT. Among those patients who did not receive PORT (n=206, 36 in A, 170 in B), group A was associated with shorter time to LR (median times to LR = 31.00±5.66 (A); 67.00±9.68 (B); log rank test, $c^2(1)=12.30$, $p<0.001$) as compared to group B. For cases with PORT (n=50, 21 in A, 29 in B), the median times to LR were 39.0±7.70 (A) and 50.00±23.70 (B) the log rank test showed no statistically significant difference, $c^2(1)=1.17$, $p=0.279$.

Conclusions: For the first time, recently suggested histopathological features of PNI were correlated with LR and time to LR in early OTSCCs. Cases with P or ET were associated with shorter time to LR only in the absence of PORT. Thus, when reporting oral tongue SCC, PNI location relative to the tumor should be reported. Larger studies with more cases may address the significance of PNI site and number of PNI foci.

1285 Head and Neck Schwannomas: A 20-Year Single Institution Experience

Randall Butler, Jonathan McHugh. University of Michigan, Ann Arbor, MI.

Background: Schwannomas are benign neoplasms that arise from Schwann cells of peripheral nerves and occur throughout the body. While the literature contains a plethora of short series and case reports describing the clinical features of head and neck (H&N) schwannomas, histopathologic data are sparse. Our aim was to examine more thoroughly the clinicopathologic characteristics of H&N schwannomas in a large series collected at a single institution.

Design: The files of our institution were searched to identify H&N schwannomas over the 20-year period 1995 to 2014, excluding cutaneous and acoustic sites. Clinical data were retrieved from the medical record, and all available routinely stained sections were retrospectively reviewed.

Results: 88 schwannomas from 85 patients, 5 with NF2, were identified; 2 tumors occurred in each of 3 patients with NF2. Across all subsites, there were 36 men (42.4%) and 49 women with a mean age of 41.3 years. The distribution of tumors was as follows: nasal cavity 4, oral cavity 9, paranasal sinuses 3, parotid gland 5, larynx 2, parapharyngeal 8, soft tissue 42, and intra/juxtaosseous 15. The most common presentation was a painless mass, (55.7%). A minority had localized symptoms (18.1% overall), although all nasal cavity tumors presented withnasal obstruction. Neurologic complaints were uncommon, but 46.7% of intra/juxtaosseous cases had such symptoms. Among cases with follow-up (76), none recurred.

85 of the tumors had slides available for review. Antoni A areas predominated over Antoni B in a majority of tumors. Schwannomas in mucosal sites were notable for a lack of encapsulation, with all tumors in the sinonasal cavityand larynx lacking a capsule. Ancient changes were common (>90%)at all sites except the oral cavity. Ulceration of mucosa or skin,was rare, occurring in 3 cases, but was observed in 2/9 oral cavity schwannomas. Intratumoral foci that resembled neurofibroma (NF) were observed in 28.2%, representing all subsites except the parapharyngeal space. Four tumors were plexiform , including 3 of 8 tumors in NF2 patients with. Pseudoglandular spaces were identified in 6 cases, including 3 of the 5 parotid tumors. No other variants were identified.

Conclusions: Schwannomas occur at subsites throughout the H&N, most commonly presenting as a painless mass and having excellent outcomes. Lack of encapsulation is a notable feature of those occurring at mucosal sites. Other unique pathologic findings in H&N schwannomas include the not infrequent occurrence of NF-like foci and pseudoglandular spaces, particularly in salivary gland tumors.

1286 Correlation of Thyroid Nodule Size By Sonography and Pathologic Exam

Allison Cavallo, Daniel Johnson, Saaduddin Saddiqui, Raymon Grogan, Peter Angelos, Edwin Kaplan, Richard DeMay, Tatjana Antic, Nicole Cipriani. University of Chicago Medical Center, Chicago, IL.

Background: Thyroid nodule size by sonography plays an important role in clinical management of thyroid lesions while nodule size at pathologic exam is central to staging of malignancies. Few studies have attempted to correlate thyroid nodule size at sonographic and pathologic examination. Bachar et al. evaluated 292 patients with solitary papillary thyroid carcinoma and observed poor size correlation, particularly for nodules larger than 1.5 cm by sonography. We attempt to characterize the relationship between thyroid nodule size at sonography and pathologic exam.

Design: We searched the archives of a large tertiary care center for all thyroid resection specimens, benign and malignant, with associated sonographic examination for the years of 2011-2013 and identified 531 nodules. Thyroid nodules at resection were correlated with those identified at ultrasound. The ultrasound size and the size at pathologic examination were recorded for each nodule. To ensure correct correlation, nodule site, size and characteristics at ultrasound were matched with nodule site and size within the gross description at resection. Nodules for which definitive correlation could not be established were excluded.

Results:

Ultrasound Size vs Gross Size of Nodule

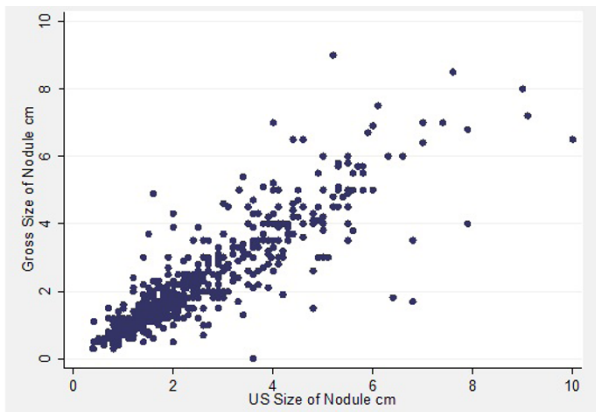

Pairwise Correlation = 0.8656 with P-value <0.00005.

Conclusions: Thyroid nodule size by sonography and pathology shows general overall correlation for benign and malignant nodules (pairwise correlation=0.87). However, for larger nodules, ultrasound and pathologic exam become increasingly discrepant, perhaps due to closely-associated or coalescent nodules measured differently at ultrasound

compared to pathologic exam. We conclude that thyroid nodule size by sonographic exam, particularly for smaller nodules, is a useful tool to guide clinical management. Size discrepancy should be taken into consideration with larger nodules, as there is a trend for ultrasound size to overestimate pathologic nodule size.

1287 Targeted Genomic Analysis of 72 Head and Neck Tumors

Sue Chang, Lynette Sholl, Jeffrey Krane, Vickie Jo. Brigham & Women's Hospital and Harvard Medical School, Boston, MA.

Background: Head and neck tumors encompass a broad range of malignancies with molecular heterogeneity within tumor types, especially squamous cell carcinoma (SCC). Preliminary data show differences in molecular profiles between conventional SCC and HPV-associated SCC (HPVSCC). This study used targeted exome sequencing to identify the frequency and types of genomic alterations in head and neck tumors.

Design: DNA was extracted from 72 formalin-fixed paraffin-embedded tumor samples and analyzed using the OncoPanel assay. OncoPanel detects somatic mutations, copy number variations (CNV), and structural variants in exonic DNA of 300 cancer-related genes and 113 introns across 35 genes for rearrangements by massive parallel sequencing using an Illumina HiSeq 2500 sequencer. MuTect and GATK were used to detect single nucleotide variants and indels, and VisCap to detect CNVs. A subset of cases also underwent breakmer analysis for structural variants.

Results: There were 23 conventional SCC, 24 HPVSCC and 15 salivary gland tumors. Five were metastatic skin SCC to intraparotid lymph nodes (LN). Other tumors were: olfactory neuroblastoma (2), NUT midline carcinoma (1), Merkel cell carcinoma (1), mucinous adenocarcinoma (1). OncoPanel detected an average of 6.7 (range, 1-73) exonic mutations across all tumors types; 55 tumors had CNVs. For SCC, the average numbers of exonic mutations were: conventional type, 6.8; HPVSCC, 4.5; metastatic conventional, 31. As expected, *TP53* mutations were observed in the majority of conventional SCC (25/28) but seen in only one case of HPVSCC. SCC showed frequent mutations in *CDK2NA*, *MLL2/3*, PI3K pathway, NOTCH family, ARID family, *PTEN*, *APC,* and *TSC1/2*. HPVSCC harbored mutations in *MLL2/3*, NOTCH, ARID, and *PTEN*, as well as mutations in *FGFR2/3, ERBB2, PTEN, ERCC4/5, DICER1*, and *PDGFRα/β*. As expected, CNVs in *CCND1, EGFR1, ATM, PTEN, PI3KA*, and *CDKN2A* were observed in all types of SCC. For salivary gland tumors, CNVs were present in nearly all cases with an average of 3.9 exonic mutations. Expected findings included *ETV6* translocation in mammary analogue secretory carcinoma (*ETV6*) and *CREBB2* mutations/alterations in adenoid cystic carcinoma.

Conclusions: A broad screening platform allows for detection of a large number of genomic events in head and neck tumors. While SCC and HPVSCC share similar genetic aberrations, differences in the spectrum of mutations were detected which may lend mechanistic insights and be of diagnostic utility. The therapeutic and prognostic significance of these findings remains to be determined, but may enable multi-tiered classification for clinical trials.

1288 Mutation Profile of Advanced Thyroid Carcinomas By Next-Generation Sequencing: The MDACC Experience

Hui Chen, Rajyalakshmi Luthra, Mark Routbort, Keyur Patel, Rajesh Singh, Hyvan Dang, Bedia Barkoh, Maria Cabanillas, Ken Aldape, Russell Broaddus, Michelle Williams. University of Texas MD Anderson Cancer Center, Houston, TX.

Background: Thyroid carcinomas have been associated with specific genetic alterations predominantly in genes encoding proteins of the RAS-RAF-MEK-ERK signaling pathway. As *BRAF* is the most common alteration, testing in isolation of this marker is often performed. Recent application of multiplex next generation sequencing to molecular diagnostics allows simultaneous testing of activating and tumor suppressor mutations in multiple signal pathways. Extended mutation profiling of advanced thyroid cancers may enhance considerations for targeted therapies.

Design: We analyzed 222 consecutive advanced thyroid carcinomas subjected to molecular profiling using next generation sequencing (NGS) on the Ion Torrent PGM (Life Technologies). We examined substitutions and small indels in 46/50 cancer-related genes using Ampliseq Cancer Hotspot v1 panel (n=187, 4/2012-8/2013) and v2 panel (n=35, 9/2013-2/2014) respectively. Sequence alignment and analysis were performed using Torrent Suite software (Life Technologies) and lab-developed software (OncoSeek). We examined the mutation status in respect to tumor morphology.

Results: Mutations were detected in 159 (72%) cases predominately in the MAPK pathway (*BRAF 49%, NRAS 11%, KRAS 4%, RET 3%, and HRAS* 2%). Additionally activating mutations in *PIK3CA* (3%), *AKT1* (1%), *ERBB2 (<1%) were detected,* and tumor suppressor gene mutations in *TP53* (6%), *RB1 (<1%), and VHL* (< 1%). *BRAF* mutation was associated with papillary carcinoma (PTC)(101/153), poorly differentiated (PD) (4/27) and anaplastic (ATC) (2/11) carcinomas. *RET* mutations were limited to medullary carcinoma (6/9). *NRAS* mutation was present in follicular (7/17) and PD (9/27) carcinomas. *TP53* mutations occurred in Hurthle carcinoma (HCC) (2/5), ATC (3/11), PD (4/27) and PTC (5/153). Of these, *TP53* was the only mutation in HCC (2/2), sometimes with co-mutation in PD (1/4) and ATC (1/3) and always co-mutation in PTC (5/5). Other common coexisting mutations were *BRAF* with *PIK3CA* (4).

Conclusions: Activating mutations in PI3 kinase pathway may be an alternative oncogenic mechanism requiring therapeutic consideration in advanced thyroid patients along with inhibiting the MAPK pathway. Additionally, *TP53* mutation may be a co-mutation or the only mutation in aggressive thyroid carcinomas requiring NGS approaches for detection.

1289 Early Squamous Cell Carcinoma of the Oral Tongue: Histologic Parameters and Local Control

Simion Chiosea, Jessica Maxwell, Yongli Shuai, Margaret Brandwein-Gensler, Bibianna Purgina, Chi Lai, Bernhard Weiss, Martin Canis, Robert Ferris, Seungwon Kim, Uma Duvvuri, Jonas Johnson, Raja Seethala, Lester Thompson. University of Pittsburgh, Pittsburgh, PA; University of Ottawa, Ottawa, Canada; University of Alabama, Birmingham, AL; University of Göttingen, Göttingen, Germany; Southern California Permanente Medical Group, Woodland Hills, CA.

Background: The significance of margins (positive *vs*. close *vs*. negative; tumor bed sampling by the surgeon *vs*. resection specimen margins taken by the pathologist) and worst pattern of invasion (WPOI) in pT1-2 pN0 squamous cell carcinomas (SCC) of the oral tongue is unclear.

Design: WPOI, distance from the invasive tumor front to the margin, the relationship between margins obtained from the tumor bed or glossectomy specimen, and other histologic parameters were assessed in 280 cases of pT1-2 pN0 SCCs of the oral tongue. Time-dependent receiver operating curves were used to assess discriminatory ability of margin width. Cases with positive margins were excluded from statistical computation of cut-off values distinguishing "close" from "negative" margin. Local recurrence (LR) was the primary endpoint.

Results: In the entire cohort of 280 cases, only the status of the margins obtained from glossectomy specimen correlated with LR (probability of being LR free at 30 months - 89% with negative margins *vs*. 75% with positive margins; $p = 0.008$). However, only a trend for such correlation is seen when analysis is limited to cases in which the tumor bed margin is sampled (n = 161). A proportional hazards regression model for margin width showed a linear relationship with a hazard ratio of 0.635 (95% confidence interval = 0.504 – 0.8) comparable to a 37% decrease in risk of LR for an increase of 1 mm of margin width (up to 5 mm; $p < 0.001$). The performance of the 3 mm margin cut-off is shown in Table 1.

Time to Local Recurrence, months	Sensitivity, %	Area Under the Curve
12	100	0.88
18	95	0.85
24	81	0.78
36	79	0.75

Sensitivity of this cut-off was highest for early recurrences and decreased over time while the specificity of 60% remained stable. While WPOI did not correlate with LR, cases with high-risk WPOI showed narrower margin clearance (3.7 mm [low risk] *vs*. 2.1 mm [high risk], mean; $p < 0.001$).

Conclusions: Only status of the margin taken from the glossectomy specimen correlates with LR. Sampling of tumor bed margins may diminish this correlation. Variable sensitivity of the 3 mm cut-off highlights heterogenous nature of cases with 0.2 to 3 mm margin width (i.e., number of close margins, difficulty to account for tumor bed margins, WPOI).

1290 Molecular Characterization of Apocrine Salivary Duct Carcinoma

Simion Chiosea, Lindsay Williams, Christopher Griffith, Victor Zota, Lester Thompson, Ilan Weinreb, Julie Bauman, Somak Roy, Raja Seethala, Marina Nikiforova. University of Pittsburgh, Pittsburgh, PA; H. Lee Moffitt Cancer Center & Research Institute, Tampa, FL; Southern California Permanente Medical Group, Woodland Hills, CA; University Health Network, Toronto, Canada.

Background: Modern classification and personalized treatment ofsalivary duct carcinomas (SDC) requires thorough molecular characterization.

Design: 30 apocrine, androgen receptor (AR) positive SDC were analyzed by Ion Ampliseq Cancer HotSpot panel V2 (Life Technologies, NY) to detect mutations in 50 cancer-related genes. *ErbB2, PTEN, FGFR1, p16, CMET, EGFR, PIK3CA* copy number changes were studied by fluorescence in situ hybridization (FISH). Findings were validated by Sanger sequencing and/or immunohistochemistry (e.g., ErbB2, p53).

Results: The five most common genetic abnormalities were as follows: *p53* mutations (including 12 missense–12/30, 40%, and 3 deletion/frame shift–3/30, 10%); *PTEN* loss (11/30, 37%, including 3 cases with *PTEN* mutation); *PIK3CA* mutations (9/30; 30%); *HRAS* mutations (8/30; 27%), and *ErbB2* amplification (8/30, 27%, including one case with *ErbB2* mutation). Two cases showed no abnormalities. There was no correlation between genetic changes and whether SDC arose *de novo* or *ex* pleomorphic adenoma. There was significant overlap between genetic changes. For instance, all cases with *ErbB2* amplification also harbored either a *p53* mutation, *PIK3CA* mutation, or *PTEN* deletion. Most cases with *PIK3CA* mutations also harbored *HRAS* mutations.

Conclusions: Based on the prevalence and type of genetic changes, as a group, apocrine SDC recapitulated the "luminal AR positive" subtype of breast carcinoma. A rational therapeutic approach may include combined inhibition of mitogen-activated protein kinase and phosphoinositide 3-kinase pathways. Variable response to conventional chemotherapy, anti-AR, or anti-ErbB2 therapy may be due to numerous overlapping genetic alterations in SDC.

1291 Are Sinonasal Hemangiopericytomas (HPCs) Sinonasal Solitary Fibrous Tumors (SFTs): STAT6 Immunohistochemistry Delineates Two Distinct, Separate Entities

Sarah Choi, Paul Zhang. Hospital of the University of Pennsylvania, Philadelphia, PA.

Background: Most soft tissue HPCs are now reclassified as SFTs, except for sinonasal HPCs, which morphologically overlap with SFTs but are regarded as a distinct entity. Nuclear STAT6 expression due to translocation has been recently used as a specific marker for SFTs. We examined STAT6 on a cohort of sinonasal HPCs to investigate the distinctness of this entity and the potential utility of this marker in establishing a more definitive diagnosis, with emphasis on equivocal cases.

Design: 11 cases of sinonasal HPCs from the sinonasal cavity from 2008-2014 were chosen. 4 cases of sinononasal SFTs were also included for comparison. STAT6 nuclear expression was evaluated immunohistochemically on paraffin section using Leica Autostainer Bond III (STAT6 polyclonal antibody, Santa Cruz Biotechnologies, S-20 sc-621, 1:200 dilution). Prior reports were also reviewed for expression of other immunohistochemical markers, in particular, CD34.

Results: Of the 11 cases of sinonasal HPCs, 3 cases demonstrated diffuse STAT6 nuclear positivity. All of these cases were also CD34 negative. Of the remaining eight cases of HPCs, three cases demonstrated focal to diffuse CD34 positivity. All four cases of sinonasal SFTs demonstrated diffuse STAT6 nuclear positivity, only two of which also were positive for CD34. Clinical follow-up of all patients, ranging from 6 months to 5 years, showed no evidence of recurrence either clinically or radiologically regardless of diagnosis.

Conclusions: If STAT6 was used as a diagnostic standard, one quarter to one third of sinonasal HPCs would be reclassified as SFTs, including those with negative CD34. This finding indicates a higher incidence of sinonasal SFTs than currently understood and highlights the utility of STAT6 as a more sensitive and specific marker of SFTs. Furthermore, nuclear STAT6 expression is significantly less frequent in sinonasal HPCs than in soft tissue HPCs/SFTs, indicating not all sinonasal HPCs are simply SFTs, and supporting the notion that sinonasal HPC, though its incidence is lower than what we expected, is a distinct entity from sinonasal SFT. STAT6 immunohistochemical stain is, therefore, essential to further differentiate SFTs from HPCs in the sinonasal tract. The clinical relevance of this distinction requires further study.

1292 Nonkeratinizing Morphology in Oropharyngeal Squamous Cell Carcinoma Implies p16 and HPV Positivity – A Four-Year Prospective Practice Study

Dikson Dibe Gondim, Wesley Haynes, Xiaowei Wang, Rebecca Chernock, Samir El-Mofty, James Lewis. Washington University, St. Louis, MO.

Background: Oropharyngeal squamous cell carcinomas (OSCC) associated with human papillomavirus (HPV) represent a distinct entity. They have differences in epidemiologic features, gene expression patterns, and most importantly, HPV status provides major prognostic information. p16 immunohistochemistry (IHC), with or without HPV-specific testing, is commonly used to assess for HPV status/prognosis. Further, many HPV-related OSCC have a distinct, nonkeratinizing morphology. We correlated the histologic typing of OSCC with both p16 IHC and HPV RTPCR in 4 years of routine clinical practice on a high volume head and neck service.

Design: Data were collected from all OSCC cases at our institution from 1/2010 to 12/2013. Primary and/or nodal metastatic tumor in all cases were typed by 3 head and neck pathologists as keratinizing (K), nonkeratinizing (NK), or nonkeratinizing with maturation (NK MAT). NK OSCC had minimal (<10% surface area) maturing squamous differentiation, NK MAT OSCC >10% maturing squamous differentiation, and K OSCC consisted entirely of tumor with maturing squamous differentiation. All were assessed for p16 IHC status with a 70% nuclear and cytoplasmic positivity cutoff as part of routine clinical practice. In addition, 70 consecutive cases were audited for high risk HPV mRNA by RT-PCR.

Results: There were 435 cases. The tumors were histologically typed without knowledge of the p16 results in 66% of the cases. The majority (90%) consisted of one of the 3 main types described and the rest (10%) of uncommon variants. Results are shown in the Table. NK morphology had 99.1% and 100.0% positive predictive value for p16 positivity and high risk HPV mRNA positivity, respectively.

OSCC type	p16 positivity	High Risk HPV RT-PCR
NK	226/228 (99.1%)	48/48 (100.0%)
K	26/114 (22.8%)	1/11 (9.1%)
NK MAT	45/49 (91.8%)	9/11 (81.8%)

Conclusions: Based on a large, 4 year, prospective study, strictly defined nonkeratinizing morphology in OSCC, which constitutes ~55% of all tumors, essentially implies positivity for both p16 IHC and transcriptionally-active high risk HPV.

1293 Transcriptionally Active Human Papilloma Virus in Sinonasal Tract Neoplasms

D Jacob Fjeldsted, Benjamin Witt, Daniel Albertson, Margaret Coppin, H Evin Gulbahce. University of Utah School of Medicine, Salt Lake City, UT; ARUP Laboratories, Salt Lake City, UT.

Background: Although it is generally accepted that prognostic significance of human papilloma virus (HPV) is confined to the squamous cell carcinomas (SCC) of the oropharynx, there is more recent literature suggesting importance of HPV in sinonasal cancers. The purpose of this study is to investigate transcriptionally active HPV as determined by in situ hybridization (ISH) in sinonasal lesions.

Design: All HPV-ISH test requests on sinonasal lesions at our national reference laboratory between January 2010 and August 2014 are identified and H&E and HPV-ISH slides were reviewed. Squamous cell carcinomas (SCC) were classified as keratinizing or nonkeratinizing following guidelines. Our laboratory offered Ventana INFORM HPV III FAMILY 16 probe for HR- HPV (type 16, 18, 31, 33, 35, 39, 45, 51, 52, 56, 58 and 66) and INFORM HPV II FAMILY 6 probe for LR- HPV (types 6 , 11). Clients had the option of ordering only HR, LR or Panel (HR+LR) testing. The vendor was switched to PathoGene (Enzo Life Sciences) high-risk HPV (types 16,18) probes in Oct-2013 and low-risk HPV (types 6,11) in Jan-2014.

Results: During the study period, 20 sinonasal lesions were submitted to our laboratory for HPV ISH testing: 10 squamous cell carcinomas (SCC) (7 for panel and 3 for HR testing), 9 sinonasal papillomas (SNP) (7 for panel, 1 for HR, and 1 for LR testing), and 1 adenoid cystic carcinoma (ACC) (for panel testing). 5/10 SCC were nonkeratinizing (NKSCC), 4/10 keratinizing (KSCC) and 1/10 was of papillary SCC phenotype. Of five NK-SCC tested for HR, 2/5 were positive and 3/5 were negative. Both of the 2 NK-SCC tested for LR were negative. All 4 K-SCC were tested for HR: 1/4 was positive, 2/4 negative, and 1/4 was indeterminate. All 4 K-SCC were also tested for LR and were negative. One papillary SCC was negative for both HR and LR. 8 of 9 SNP (4 inverted, 1 with high-grade dysplasia) were tested for LR and 3/8 were positive. 8/9 SNP were tested for HR HPV (including one with high grade dysplasia) and all were negative. One case of ACC was negative for both LR and HR.

Conclusions: 30% of sinonasal SCC are HR HPV positive by ISH. By contrast, no sinonasal papillomas in our study were associated with high risk HPV by ISH. A significant proportion (40%) of SCC in this location is of keratinizing type. If significance of HPV infections in outcome for sinonasal SCC is confirmed with further studies, testing all types of SCC in this anatomic location may be needed.

1294 Capillary Hemangioma of Nasal Type: Clinicopathological Study of 13 Cases of a Distinctive and Potentially Confusing Hemangioma Variant

Ruifeng Guo, Andrew Folpe. Mayo Clinic, Rochester, MN.

Background: Capillary hemangiomas (CH) are common, benign neoplasms of endothelial cells, typically consisting of well-formed, capillary-sized vessels growing in a distinctly lobular pattern. The diagnosis of most CH is straightforward. Some CH are, however, more challenging diagnostically owing to atypical features such as high cellularity (e.g., infantile hemangioma) or non-lobular growth pattern (e.g, anastamosing hemangioma). Over the past several years we have seen in consultation a distinctive CH of the nasal cavity, provisionally termed "CH of nasal type" (CH-NT), which is frequently confused with a variety of potentially more aggressive lesions.

Design: Available slides from 13 cases coded as "CH-NT" were retrieved from our archives. Immunostains to CD31, CD34 and smooth muscle actin (SMA) were performed in selected cases. Submitting diagnoses included: "query angiofibroma, r/o malignancy" (N=4), "vascular polyp, r/o malignancy" (N=3), "query malignant vascular tumor" (N=4), "sinonasal hemangiopericytoma" (N=1), and "benign vascular tumor" (N=1). Follow-up information was obtained.

Results: The patients (10M, 3F) ranged from 6 to 57 years of age (median 44). Available radiographic studies often showed worrisome features including erosion of facial bones and nasal septa. The tumors ranged from 1.1 cm-6.0 cm. Microscopically, the tumors showed striking stromal edema and myxoid change, which obscured the underlying lobular capillary arrangement. Within this myxoid matrix, a florid capillary proliferation was present, frequently with non-atypical mitotic activity. In some instances a branching, "hemangiopericytoma-like" vascular pattern was present in areas. The overall cellularity was low to moderate, and endothelial atypia or hyperchromatism was absent. Immunostains to CD31, CD34 and SMA highlighted areas of lobular growth pattern inapparent on the routinely stained slides. Follow-up (N=9, 11-96 months, median 73 months) revealed no local recurrences or metastases.

Conclusions: CH-NT is a distinctive CH variant with unusual clinicopathological features, including bone erosion, prominent myxoid change, lack of a well-defined lobular growth pattern, and mitotic activity, often raising concern for a more aggressive endothelial process, or a non-endothelial tumor. The distinctive morphological features of CH-NT may be related to its location within a hollow cavity. Awareness of this distinctive CH variant and the use of ancillary immuonstains to highlight its lobular growth pattern should facilitate confident diagnosis in most instances.

1295 PAX3 Rearrangement in Low-Grade Sinonasal Sarcoma With Neural and Myogenic Differentiation (LGSSNMF): An Ancillary Molecular Diagnostic Tool for a Recently Described Entity

Juan Hernandez-Prera, Ricky Kwan, Alessandro Valentino, Vesna Najfeld, Bruce Wenig. Mount Sinai Health System, New York, NY.

Background: LGSSNMF is a distinct recently described sinonasal sarcoma characterized by concomitant neural and myogenic differentiation by immunohistochemistry and the presence of a recurrent PAX3-MAML3 gene fusion. Herein, we present a series of LGSSNMF and evaluate the utility of PAX3 rearrangement as adjunct molecular test in its diagnosis.

Design: Institutional pathology records and the consults files of one of the authors were searched for cases morphologically and immunohistochemically compatible with LGSSNMF. Six LGSSNMF were collected. Clinical information was available for 5 of the 6 cases; 1 consult case lacked demographic and clinical information. All identified cases were reviewed and subjected to fluorescence in situ hybridization (FISH) on paraffin sections using a commercially available PAX3 dual-color break-apart probe (Cytocell, Cambridge, UK). Data was collected and collated.

Results: There were 4 women and 1 man, with a mean age of 58 years (range 36-66). Two cases occurred in the nasal cavity, 1 case arose in ethmoid sinus, 1 case involved the nasal cavity and ethmoid and 1 case involved the nasal cavity with invasion of the orbit and base of skull. The tumors were characterized by a submucosal unencapsulated cellular spindle cell proliferation with a fascicular to storiform growth. The spindle

cell proliferation was uniform and intimately associated with invaginations of surface respiratory epithelium. Rare mitotic figures were seen and necrosis was absent. All tumors showed variable expression for S-100 and smooth muscle actin. FISH testing was technically inadequate in 2 cases. In the 4 cases available for FISH testing, PAX3 rearrangements were detected in 30-80% of 200 interface nuclei. Long term follow up was available in 2 cases. These patients were alive with no evidence of disease after 16 and 3 years follow-up.
Conclusions: Our study contributes to the number of reported cases of LGSSNMF in the literature reaffirming this entity as a unique sinonasal neoplasm. We also confirm the presence of PAX3 rearrangement by FISH in 4/4 cases validating its utility in the diagnosis of LGSSNMF. Owing to its characteristic histologic, immunohistochemical and molecular features, LGSSNMF is a distinct sinonasal neoplasm separate from low-grade malignant peripheral nerve sheath tumor or a myogenic sarcoma.

1296 Sinonasal Oncocytic Glandular Neoplasm With Retained Myoepithelial Cells: Reappraising the Benign Versus Malignant Paradigm

Juan Hernandez-Prera, Alessandro Valentino, Beverly Wang, Paul Wakely, Tony Ng, Kenneth Berean, Bruce Wenig. Mount Sinai Health System, New York, NY; Ohio State University, Columbus, OH; University of British Columbia, Vancouver, Canada.
Background: WHO classification regards all sinonasal glandular neoplasms lacking features of salivary gland tumors as adenocarcinomas with no benign counterpart. We present a series of a non-salivary glandular neoplasm that challenges prior tumor definition in this anatomic area.
Design: 4 non-salivary sinonasal glandular neoplasms with oncocytic cytomorphology with retained myoepithelial cells were identified from our files and reviewed. PAS-D and immunohistochemical (IHC) stains including AE1/AE3, p63, S100, calponin, smooth muscle actin (SMA), Ki-67, CK20, CDX2, and SOX-10 were performed. Clinical parameters were obtained.
Results: All patients were men, with a mean age of 67 years (range 59-73). 3 cases occurred in the nasal cavity and one in the maxillary sinus. Mean tumor size was 2.4 cm (range 1.6-4 cm). 3 cases were asymptomatic and discovered during imaging studies for unrelated conditions; 1 patient presented with epistaxis, dry nose, and epiphora. All tumors were unencapsulated and submucosal with complex growth (i.e., back-to-back glands) lacking intervening stroma. The glands were comprised of cells with of oncocytic cytoplasm and uniform round to oval nuclei. An outer layer of flat to low cuboidal cells was variably identified. There was mild nuclear pleomorphism, rare mitotic figures and no necrosis. Invasive growth was not identified although bone erosion was present. Direct continuity to surface epithelium was evident in 2 cases. Intraluminal DPAS-positive material was present. All cell types were positive for AE1/AE3 with variable SOX10 staining; p63, S100, calponin, SMA highlighted the outer cell layer; CK20 and CDX2 were negative. A proliferation rate of <5% was seen by Ki67 staining. All tumors were removed surgically and all patients were alive with no evidence of recurrence or metastasis after a mean follow up of 14 months.
Conclusions: The findings in our cases show features described for low grade sinonasal adenocarcinoma. However, the presence of myoepithelial cells suggests a possible diagnosis of an adenoma. Defining these tumors as "adenomas" seems justified, yet this diagnostic term is not recognized and the designation of "low grade adenocarcinoma" has been historically preferred and is the one we advocate using. We believe our cases represent a heretofore poorly recognized entity meriting distinction from other sinonasal glandular lesions and neoplasms, including hamartomas.

1297 Correlation of p16 Staining Pattern With HPV Genotypes and Histology in Head and Neck Squamous Cell Carcinomas

Junaid Ibrahim, Luis Perez-Casanova, Huazhang Guo, Miao Cui, Aneta Waluszko, Fei Ye, Janina Longtine, David Zhang. Mount Sinai St. Luke's – Roosevelt Hospital, New York, NY; Bellvitge University Hospital, L'Hospitalet de Llobregat, Barcelona, Spain; Mount Sinai Hospital, New York, NY.
Background: Human papillomavirus (HPV) related squamous cell carcinomas (SCC) of head and neck region are increasing in incidence and have a better prognosis than non-HPV related SCC. p16 immunostaining is commonly used as a predictor of HPV status, especially in positive or negative results. The aim of this study is to specify the predictive value of p16 in correlation with histology.
Design: We retrieved SCC cases since 2012 with molecular HPV study (real-time PCR for HPV 16/18 or Sanger Sequencing for non-HPV 16/18 genotypes) and p16 staining. SCC were subcategorized into keratinizing (KSCC), non-keratinizing (NKSCC), hybrid (HSCC), basaloid (BSCC) and not specified (SCC NOS). p16 was reported as positive, focal or negative.
Results: A total of 418 cases were studied, 211 were HPV+ (189 HPV16, 6 HPV18, 3 HPV33, 10 HPV35, 3 HPV45) and 207 were HPV-.
HPV16 and 18 were equally distributed among all subcategories of SCC, while other high risk genotypes were more common in subcategories other than KSCC.
Overall sensitivity for p16 was 90% (189/211) and specificity was 75% (155/207).

	P16 POSITIVE (214)		P16 FOCAL (42)			P16 NEGATIVE (162)	
P16 / HPV	Total p16+	HPV +	Total focal p16	HPV-	HPV+	Total p16-	HPV-
KSCC	42	31	22	18	4	107	106
NKSCC	80	78	7	3	4	9	6
HSCC	24	20	4	2	2	3	3
SCC NOS	56	50	9	4	5	41	38
BSCC	12	10	0	0	0	2	2

p16 was positive in 83% of NKSCC, 77% of HSCC, 85% of BSCC and in only 25% of KSCC. 99% of p16- KSCC were HPV-. 35% of all focal staining cases were HPV+ (18% of focal staining KSCC and 57% of focal staining NKSCC). BSCC didn't show focal staining. All p16 focal staining HPV+ cases were HPV16 genotype.
Conclusions: p16 had a 99% negative predictive value and a 74% positive predictive value in KSCC and a 97.5% positive predictive value in NKSCC. p16 positive KSCC should be confirmed with molecular HPV test. p16 focal staining cases need molecular HPV test regardless of histology. Histological correlation is needed when evaluating p16 staining.

1298 Prognostic Factors in Carcinoma Ex Pleomorphic Adenoma

Omar Jaber, Robert Robinson. University of Iowa, Iowa City, IA.
Background: Carcinoma ex pleomorphic adenoma (CEPA) is defined as a malignant epithelial neoplasm arising from a pleomorphic adenoma. CEPA has been prognostically subclassified according to invasion of the tumor capsule, with no invasion termed non-invasive (in situ), <= 1.5 mm termed minimally invasive and >1.5 mm as invasive. The prognosis is thought to be excellent for the first two while the latter is thought to have a worse prognosis. However, other studies have suggested a higher threshold for invasion, including 5, 6 or 8 mm. In addition, the tumor grade has been thought to have a prognostic role, especially in the invasive carcinomas. Proliferation index (PI), vascular and perineural invasion and lymph node status are also suggested to be prognostic factors. To further explore these topics we reviewed a series of CEPA studying the correlation between these variables and prognosis, especially for non-invasive, minimally invasive and invasive subtypes.
Design: Departmental files were searched between 1990 and 2014. 34 cases of CEPA were identified, of which 23 cases had adequate followup with 18 of these available for Ki67 staining to assess PI. Capsular invasion, histologic subtype and grade of malignancy, lymphovascular invasion (LVI), perineural invasion (PNI) and lymph node status were assessed. Capsular invasion was measured (in mm) using a calibrated objective. PI was assessed counting 1000 cells.
Results: 13 of the 23 patients had non-invasive tumors and 4 had minimally invasive tumors. No recurrence or death were seen with non-invasive or minimally invasive disease even when the malignant component had a high histologic grade and high PI. Six patients had capsular invasion beyond 1.5mm. Of these, 3 patients had no recurrent disease and are well. None of the these patients had LVI, PNI or lymph node metastases. Of the 3 others, one patient had a recurrence after one year and two patients died of disease. Both patients who died had LVI, PNI and positive lymph nodes at time of diagnosis. The one patient with recurrence had no LVI or PNI but had a tumor that was deeply invasive into the surrounding fat. PI correlated with tumor grade rather than capsular invasion.
Conclusions: In this series, patients with CEPA that were non-invasive or minimally invasive all had good outcome. However, patients having greater than 1.5 mm invasion beyond the capsule only had a fatal outcome if there was concomitant LVI, PNI and lymph node metastases. Higher tumor grade and high PI was not associated with worse prognosis.

1299 Epigenetic Modulation Significantly Enhanced EGFR-Targeted Killing of HNSCC Cells

Shahanawaz Jiwani, Haihong Zhang, Lingbao Ai, Emre Vural, Chun-Yang Fan. University of Arkansas for Medical Sciences, Little Rock, AR; University of Florida, Gainesville, FL; Central Arkansas Veterans Healthcare System, Little Rock, AR.
Background: Epidermal Growth Factor Receptor (EGFR) signaling pathway is critically involved in the pathogenesis of head and neck squamous cell carcinomas (HNSCC) and there has been immense interest in exploring targeted therapies aiming at EGFR, using specific EGFR tyrosine kinase inhibitors, such as Gefitinib (Iressa). Suppressor of cytokine signaling 1 (SOCS1) is an effective, negative regulator of the EGFR signaling pathway. In this study, we attempt to investigate whether epigenetic modulation by demethylation of key genes in EGFR signaling pathway will influence the efficacy of EGFR-targeted killing of HNSCC cells.
Design: A HNSCC cell line (T409) that was previously shown by us to contain hypermethylated SOCS1 gene was used in the study. The cultured cancer cells were exposed to 5-azacytidine (5-AC), a DNA demethylating agent, in culture media at concentrations ranging from 0 to 8 μM and simultaneously exposed to Iressa, an EGFR tyrosine kinase inhibitor, at concentrations ranging from 0 to 100 μM for 7 days, followed by determination of cell viability using trypan blue enumeration assay. Inhibition of cancer cell proliferation was analyzed using various statistical models.
Results: Iressa showed a dose-dependent inhibition of the cultured HNSCC cells at biologically achievable doses (less than 10 μM) with an IC50 of 2.36 μM in the absence of 5-AC and IC50 of 1.06 μM, 1.28 μM and 0.67 μM in the presence of 5-AC at the concentrations of 2, 4 and 8 μM respectively. As a single agent, 4 μM 5-AC, 0.1 μM and 1 μM Iressa inhibited 17%, 5% and 45% HNSCC cells respectively. By contrast, the combined 4 μM 5-AC/0.1 μM Iressa and 4 μM 5-AC/1 μM Iressa treatments inhibited 28% and 50% cancer cell growth respectively. The differences in cancer inhibition between single agent treatment (Iressa at 0.1 and 1 μM) and two-agent treatment (4 μM 5-AC/0.1 μM Iressa and 4 μM 5-AC/1 μM Iressa) were statistically very significant ($p < 0.001$ and $p = 0.001$ respectively).
Conclusions: In the presence of 5-AC, a DNA demethylating agent, which works to reactivate SOCS1 gene, a negative regulator of the EGFR signaling pathway, HNSCC cancer cells are greatly sensitized to the killing effects by Iressa, a specific inhibitor of EGFR tyrosine kinase.

1300 Nuclear Expression of β-Catenin is Specific for Basal Cell Adenomas of the Salivary Gland

Vickie Jo, Jeffrey Krane. Brigham & Women's Hospital and Harvard Medical School, Boston, MA.

Background: The differential diagnosis for basaloid neoplasms of the salivary gland can be challenging. Limited published data have reported that approximately half of basal cell adenomas harbor *CTNNB1* mutations, and that nuclear β-catenin expression is prevalent. This study aimed to evaluate the extent of nuclear expression in basal cell adenomas in comparison to other common salivary gland tumors.

Design: Cases were retrieved from surgical archives. Immunohistochemical staining for β-catenin was performed on FFPE whole-sections using a mouse monoclonal antibody (BD Bioscience, #610154) at a 1:1000 dilution with antigen retrieval by citrate buffer and pressure cook. Appropriate positive and negative controls were used. Nuclear staining was recorded as positive (0/negative, no staining; 1+/focal, <10%, 2+/multifocal, 25%-75%; 3+/diffuse, >75%) and intensity of staining (graded as weak, moderate, and strong).

Results: Nuclear β-catenin staining was present in 12/16 (75%) of basal cell adenomas, and was negative in 1 case of basal cell adenocarcinoma. Most positive cases showed diffuse and strong nuclear staining, predominantly in the basal component. No nuclear staining was observed in adenoid cystic carcinoma (0/13) or pleomorphic adenoma (0/10). 1/2 cases of epithelial-myoepithelial carcinoma showed focal weak nuclear staining. Most tumors showed diffuse membranous staining in the absence of nuclear staining (including the negative basal cell adenomas).

Conclusions: While nuclear β-catenin expression has moderate sensitivity (75%) for basal cell adenoma, specificity is high (96%). The characteristic nuclear staining pattern may be useful in the differential diagnosis of basaloid neoplasms, especially in small biopsy or FNA samples.

1301 Detection of Cutaneous Human Papillomavirus Genus Beta (HPV β) mRNA Expression in Morphologically and Immunohistochemically Distinct Subsets of Squamous Carcinoma Precursor Lesions in Organ Transplant Recipients

D Anand Rajan Kanagasabapathy, Rebecca Chernock, James Lewis, Jr, Samir El-Mofty. Washington University School of Medicine, St. Louis, MO.

Background: HPV β DNA is more frequently identified in cutaneous squamous cell carcinoma (SCC) in immunosuppressed organ transplant recipients (OTR) as compared to immune competent individuals. Yet, some studies fail to detect viral mRNA expression in invasive cancer, suggesting a hit-and-run mode of carcinogenesis. We recently identified two distinct SCC precursor lesions in a cohort of transplant recipients which we termed bowenoid and nonbowenoid types of dysplasia (BD and NBD). Here we investigate the nature of expression of HPV β E6/E7 mRNA in the cohort by in-situ hybridization (ISH) using an assay with probes for 25 HPV β types.

Design: We assembled 60 paraffin embedded tissue cores (1.5 mm) from skin biopsies of 40 organ transplant recipients (age: 26-84 yrs; M:F 4.5:1) in two tissue microarrays (TMAs). These included BD (n=33) and NBD (n=17) lesions and controls from adjacent skin (n=10, 5 from each). A novel ISH RNAScope assay with probes for 25 HPV β types was used to test for E6/E7 transcripts. Probes were applied in two pools, the first for HPV β 5, 8, 9, 12, 14, 15, 17, 19, 20, 21, 22, 23, 24, and the second for types 25, 36, 37, 38, 47, 49, 75, 76, 80, 92, 92 and 96. Positive loci were enumerated (per 3.5 mm^2 area) on 400x whole-slide scanned images and expression levels were compared across groups.

Results: Hybridization signals were evident as small brown dots 1-3 per cell, predominantly localized to the nucleus. Positive nuclei were seen consistently in the suprabasal zones. Increased positive cells were encountered in BD compared to NBD and controls which exhibited far fewer positivity. Mean (95% CI) positive loci were 20.7 (12.5 - 30) and 14.08 (10 - 18.25) in BD, compared to 4.5 (0 - 8.3) and 2.2 (0 - 4.4) in controls and 9 (4.4 - 13.6) and 4.5 (2.2 - 8.5) in NBD. Differences were statistically significant ($p = 0.006$, BD vs controls & BD vs NBD, student t-test).

Conclusions: These observations suggest that HPV β may play a significant role in the pathogenesis of some, but not all premalignant cutaneous lesions in OTRs and most likely in their progression to invasive SCC. Unlike mucosal HPV α, low level lesional transcript expression is seen with cutaneous HPV β. Confirmation and further characterization of molecular pathogenetic mechanisms may be useful in identification of specific targets for therapeutic management without compromising immunosuppression.

1302 Solitary Fibrous Tumors of the Head and Neck: Clinicopathological, Immunohistochemical and Molecular Characterization of 33 Cases

Yu-Chien Kao, Hui-Chun Tai, Shih-Chiang Huang, Chien-Feng Li, Jen-Wei Tsai, Jui Lan, Hsuan-Ying Huang. Shuang Ho Hospital, Taipei Medical University, Taipei, Taiwan; Changhua Christian Hospital, Changhua, Taiwan; Chang Gung Memorial Hospital, Taoyuan, Taiwan; Chi Mei Medical Center, Tainan, Taiwan; E-Da Hospital, Kaohsiung, Taiwan; Chang Gung Memorial Hospital, Kaohsiung, Taiwan.

Background: Solitary fibrous tumors (SFTs) is a fibroblastic neoplasm of ubiquitous anatomical distribution. However, SFTs involving affecting the head and neck remain to be specifically elucidated, especially in the characterization of hallmark inv12(q13q13)-derived *NAB2-STAT6* fusion and the resultant STAT6 nuclear relocation.

Design: Together with 28 site-relevant histological mimics categorized into 13 entities, 33 head and neck SFTs were analyzed for immunoexpression and subcellular localization of STAT6, histopathological variations, and clinical outcomes. *NAB2-STAT6* fusion was determined by RT-PCR for 16 SFTs with assessable RNAs.

Results: Sixteen males and 17 females, aged between 13 and 79 years (median, 47), had primary SFTs ranging from 0.5 to 8 cm (median, 2.5) and originating in the oral cavity/pharynx (n=9), orbit (n=9), somatic soft tissues and skull bone (n=8), and sinonasal structures (n=7). Among the SFTs without adverse outcomes, 18 were histologically typical with fibrosclerotic stroma, 5 giant cell angiofibroma-like (4 orbital; 1 nasal), 5 cellular/atypical, and 1 fat-forming. Two of the 4 histologically malignant cases, including one with precedent local recurrence, developed metastases to the abdomen and lung at 13.5 and 15.5 years, respectively. Without nuclear staining in histological mimics, STAT6 distinctively labeled the tumoral nuclei in 32 (97.0%) SFTs with moderate to strong intensity. Twelve (75%) SFTs exhibited *NAB2-STAT6* fusions of heterogeneous exon composition, including the exon 4-2 in 3 cases, 4-4, 6-16, and 6-17 in 2 each, and 2-2, 3-19, and 7-17 in 1 each, while 4 nuclear STAT6-positive cases failed to be detected.

Conclusions: Considerable heterogeneity exists in the head and neck SFTs, regarding the sites of occurrence, histological patterns, and clinical behavior. Nuclear STAT6 immunoexpression is diagnostically sensitive and specific to distinguish from mimics. Although RT-PCR is a confirmatory diagnostics, SFTs in this region harbor various *NAB2-STAT6* fusions of heterogeneous composition, perhaps including undetected miscellaneous fusion variants.

1303 PLAG1 Immunohistochemistry Is a Sensitive Marker for Pleomorphic Adenoma: A Comparative Study With PLAG1 Genetic Abnormalities

Nora Katabi, Achim Jungbluth, Lei Zhang, Yun-Shao Sung, Ronald Ghossein, Cristina Antonescu. Memorial Sloan Kettering Cancer Center, New York, NY.

Background: *PLAG1* is a proto-oncogene frequently rearranged in pleomorphic adenoma (PA), resulting in overexpression of PLAG1 protein. PA has a broad spectrum of histologic features and can mimic many malignant salivary gland tumors. The aim of this study is to evaluate the sensitivity and specificity of PLAG1 immunohistochemistry (IHC) in the differential diagnosis of PA. IHC results were then compared to *PLAG1* gene abnormalities detected by FISH.

Design: PLAG1 immunostaining was performed in 82 salivary gland tumors including 23 PA, 15 carcinoma ex-PA (CA ex-PA), and 44 other types of tumors. PLAG1 staining of ≤ 5% was considered as negative. In addition, *PLAG1* FISH was performed in 44 cases for the presence of gene rearrangements/amplifications.

Results: The results of PLAG1 IHC and FISH are displayed below showing high sensitivity of PLAG1 IHC in 96% of PA; however discordant results were noted between PLAG1 FISH abnormalities and IHC in 13/44 cases (29%). Three de novo MECA and 1 BACA were negative for FISH but positive for IHC; while 2 CA ex-PA were positive for FISH but negative for IHC. PLAG1 IHC can differentiate CA ex-PA from de novo SDC, but not from de novo MECA (p=0.02).

	PLAG1 IHC*	PLAG1 FISH*
PA	22/23 (96%)	5/15 (33%)
CA ex-PA	10/15 (67%)	10/12 (83%)
Salivary duct carcinoma (SDC) de novo	0/6	0/3
Myepithelial carcinoma (MECA) de novo	7/10 (70%)	0/6
Basal cell adenocarcinoma (BACA)	3/4 (75%)	0/2
Polymorphous low grade adenocarcinoma (PLGA)	0/8	0/6
Epithelial-myoepithelial carcinoma	2/2 (100%)	ND
Mucoepidermoid carcinoma	1/4 (25%)	ND
Adenoid cystic carcinoma	0/5	ND
Acinic cell carcinoma	0/5	ND
Mammary analogue secretory carcinoma	0/1	ND
*: number of positive/total number. ND: not done		

Conclusions: PLAG1 IHC is a sensitive marker for PA, and may point to PLAG1 gene abnormalities beyond FISH resolution. Thus a negative PLAG1 IHC might be helpful in excluding a PA diagnosis. Interestingly in the context of Ca-ex PA FISH is more sensitive than IHC in detecting PLAG1 abnormalities.

1304 Determining the Prevalence of High-Grade Transformation in Acinic Cell Carcinoma in the Era of Mammary Analogue Secretory Carcinoma of Salivary Glands

Michael Keeney, Ashish Chintakuntlawar, Michael Rivera, David Schembri Wismayer, Jean Lewis, Katharine Price, Joaquin Garcia. Mayo Clinic, Rochester, MN.

Background: Our insight into the biology of acinic cell carcinoma (AcCC) has improved with the recent characterization of mammary analogue secretory carcinoma of salivary glands (MASC). Unlike AcCC, MASC is characterized by the *ETV6-NRTK3* fusion transcript. Considering the histomorphologic overlap between AcCC and MASC, it is not surprising that a significant portion of MASC cases were previously classified as AcCC. To accurately depict the incidence of high-grade transformation in AcCC (AcCC-HGT), investigational studies must exclude morphologic mimics such as MASC. Herein, we describe the prevalence of AcCC-HGT in a series of cases of AcCC with intact *ETV6*.

Design: Retrospective clinical and histopathologic review was performed on 54 patients with AcCC who had surgery at our institution from 1985-2010. Cases were classified as AcCC, AcCC-HGT, or MASC. Fluorescence in situ hybridization (FISH) was performed on all cases using a break-apart *ETV6* probe. Cases with *ETV6* rearrangement were tested for the *ETV6-NRTK3* fusion transcript using reverse transcriptase-polymerase chain reaction (RT-PCR). Five year recurrence free survival (RFS) and overall survival (OS) were calculated using the Kaplan-Meir method for AcCC and AcCC-HGT.

Results: Six of the 54 cases demonstrated *ETV6* rearrangement, harbored an *ETV6-NTRK3* fusion transcript, and were consequently excluded from this study. Of the 48

cases included in the study, 8 (17%) were classified as AcCC-HGT and 40 (83%) as AcCC. AcCC-HGT cases showed a 5-year RFS of 12% (95% CI; 0-35%), compared to 80% (95% CI; 66-95%) in AcCC cases (HR 14, P<0.0001). The-5 year OS was 43% (95% CI, 6-79%) in AcCC-HGT cases, compared to 97% (95% CI, 92-100%) in AcCC cases (HR 9, P<0.0001).

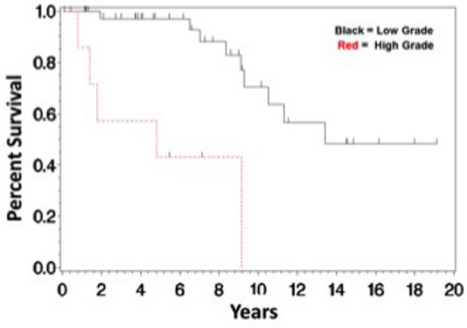

Conclusions: In this study, we determine the prevalence of high-grade transformation in cases of AcCC. In light of the recent discovery and characterization of MASC, excluding it from studies of AcCC will facilitate our understanding of the pathogenesis of AcCC.

1305 Finding HPV-Related Carcinoma With Adenoid Cystic-Like Features of the Sinonasal Tract Among a Series of Previously Diagnosed Adenoid Cystic Carcinomas

Christina Kovacs, Oleksander Kryvenko, Jennifer Chapman, Carmen Gomez-Fernandez. Jackson Memorial Hospital, Miami, FL; University of Miami Miller School of Medicine, Miami, FL.

Background: HPV-related carcinoma with adenoid cystic-like features of the sinonasal tract is a newly described entity. This neoplasm shares morphologic features with true adenoid cystic carcinoma of salivary gland. It is characterized by a cellular proliferation of pleomorphic basaloid cells with predominantly solid architecture, in addition to surface epithelial squamous dysplasia and diffuse positivity for p16. The aim of this study was to identify additional cases of this newly described cancer.

Design: We retrospectively analyzed cases from a single institution diagnosed as adenoid cystic carcinoma in the sinonasal area between June 2006 and September 2014. Of 26 cases identified, 13 had material available for review. Subsequent staining with p16 was performed on all cases. Morphology, p16 IHC results, clinical histories and outcome were reviewed.

Results: Five cases of HPV-related carcinomas with adenoid cystic-like features were identified. Patients ranged in age from 33 to 48 years old and four cases occurred in women. These tumors were characterized by a pleomorphic basaloid cell population arranged primarily in solid rounded nests separated by a variably hypocellular stroma. Focal cribriform architecture demonstrated basaloid cells arranged around microcystic spaces. Tumor nuclei were pleomorphic, oblong and hyperchromatic. Mitotic activity ranged from 1-10/HPF. Common to 4 cases was the presence of surface epithelial dysplasia. One case did not have a surface component sampled. In 2 of the 4 cases the carcinomas were directly continuous with the surface dysplasia. IHC for p16 was diffusely positive in all 5 cases, as compared with the selective staining of the cells lining the ductal structures observed in true adenoid cystic carcinomas. The surface epithelial dysplasia was likewise positive for p16. Of note, 2 of the 5 cases were associated with sinonasal inverted papillomas.

Conclusions: HPV related adenoid cystic-like carcinoma of the sinonasal cavity is associated with surface epithelial dysplasia, basaloid and cribriform morphology and diffuse p16 positivity. When encountering sinonasal carcinoma with adenoid cystic-like morphology, particular attention should be paid to the surface epithelium for the presence of epithelial dysplasia, as this appears to be a defining feature of HPV-related carcinoma with adenoid cystic-like features of the sinonasal tract.

1306 CD8 Dominant Tumor Immune Infiltrate Together With Aerobic/Glucose-Independent Tumor Metabolism Correlate With Improved Response To Radiotherapy in Head and Neck Squamous Cell Carcinoma

Rosemarie Krupar, Ravi Pathak, Andrew Sikora, Ferdinand Hofstaedter, Anja Bosserhoff, Matthias Hautmann. Baylor College of Medicine, Houston, TX; Universitaet Regensburg, Regensburg, Germany; Universitaetsklinikum Regensburg, Regensburg, Germany.

Background: Besides mutational status, tumor immune microenvironment and metabolism are major determining factors of radioresponse in head and neck squamous cell carcinoma (HNSCC). While a strong CD8 dominant immune infiltrate supports radiosensitivity, anaerobic tumor metabolism due to hypoxia contributes to radioresistence and immunosuppression. This study aimed to incorporate immunologic and metabolic markers to predict radiation response in HNSCC treated by primary radiochemotherapy (RCT).

Design: Pretreatment biopsies of 74 HNSCC were immunohistochemically analyzed for T cell subtype infiltration (CD8, CD4) and expression of proteins involved in anaerobic (GLUT1) and aerobic (COX5B) metabolism. Mean lymphocyte count in 5 high power fields and H-score (0–300) of metabolic markers were assessed by one pathologist blinded to clinical data. Results were correlated with short term survival (12 months), corresponding to therapy response, and long term survival (60 months) by Kaplan-Meier survival analyses.

Results: CD8/CD4 was decreased in GLUT1 high (p=0.021) and increased in COX5B high tumors (p=0.075) indicating an immunosuppressive microenvironment in anaerobic and immuno-permissive microenvironment in aerobic tumors. Increased CD8/CD4 was associated with a trend towards better short term (p=0.074), but not long term survival. Incorporating metabolic markers into survival analyses gave the best prediction of therapy response with improved short term survival in tumors with high CD8/CD4 and high COX5B (p=0.063) or high CD8/CD4 and low GLUT1 (0.046). There was no difference in long term survival for the marker combinations.

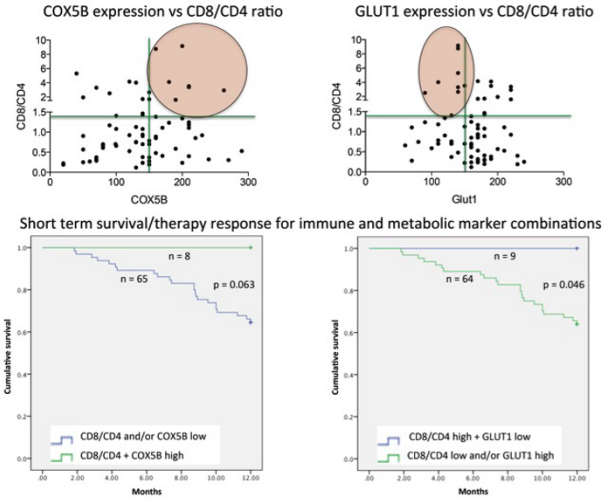

Conclusions: Aerobic/glucose-independent tumor metabolism is closely related to CD8 dominant immune infiltrate and in combination improves response to RCT in HNSCC. Facilitated activation of antitumoral immune response by RCT due to aerobic tumor energy metabolism might represent an important underlying mechanism of radiation sensitivity.

1307 Spindle Cell Lipoma of the Tongue: A Clinicopathologic Study of 8 Cases

Sean Lau, Justin Bishop, Lester Thompson. Southern California Permanente Medical Group, Woodland Hills, CA; Johns Hopkins Medical Institutions, Baltimore, MD; Southern California Permanente Medical Group, Anaheim, CA.

Background: Spindle cell lipoma is a histologically distinct variant of lipoma characteristically arising in the subcutis of the posterior neck, upper back, or shoulder. Spindle cell lipomas are uncommon within the oral cavity and rare in the tongue.

Design: Eight cases of spindle cell lipoma affecting the tongue were retrospectively reviewed. Morphologic features, immunohistochemical characteristics, and outcome data were analyzed.

Results: The study group included five men and three women ranging in age from 35 to 80 years (mean 57 years). Most lesions presented as either a painless or slowly growing lingual mass. The tumors were well circumscribed and characterized microscopically by a mixture of mature adipocytes, cytologically bland spindle cells, and interspersed bundles of thick collagen fibers in variable proportions. Myxoid stroma was a prominent feature in three lesions. Two of the myxoid predominant lesions exhibited foci comprised of small, multivacuolated adipocytes, imparting a chondroid lipoma-like appearance. By immunohistochemistry, the lesional spindle cells were strongly immunoreactive for CD34 in all tumors evaluated (7/7) and negative for S-100 protein (0/7), desmin (0/6) and smooth muscle actin (0/6). Treatment consisted of local excision in all cases. There have been no recurrences to date, with clinical follow up information available for all patients (range 11-118 months; mean 50.8 months).

Conclusions: Spindle cell lipomas of the tongue are rare, and should be distinguished from other fat containing spindle cell neoplasms that can arise at this anatomic site. Lingual spindle cell lipoma follows a benign clinical course without risk of recurrence.

1308 Human Papillomavirus DNA, HPVE6*1 mRNA and Related Molecular Markers in Over 4000 Head and Neck Squamous Cell Carcinomas

Belen Lloveras, Laia Alemany, Dana Holzinger, Silvia de Sanjose, Omar Clavero, Llucia Alos, Ignacio Bravo, Beatriz Quiros, Maria Alejo, Sara Tous, Marisa Mena, Wim Quint, Michael Pawlita, Nubia Munoz, Francesc Xavier Bosch, Xavier Castellsague. Hospital del Mar, Barcelona, Spain; Catalan Insitute of Oncology, IDIBELL, Barcelona, Spain; CIBERESP, Madrid, Spain; DKFZ Institute, Heidelberg, Germany; Hospital Clínic, Barcelona, Spain; Hospital General de l'Hospitalet, Barcelona, Spain; DDL Diagnostic Laboratory, Rijswijk, Netherlands.

Background: Human papillomavirus (HPV) is involved in a subset of head and neck squamous cell carcinomas (HNC). However, according to published data, the proportion in each country and in different anatomical site varies. This studyexplores the HPV DNA prevalence and type distribution in HNC worldwide.

Design: Paraffin embedded tumors from oral cavity, pharynx and larynx were collected from 32 countries. After histopathological evaluation, HPV DNA detection was performed using SPF-10 PCR/DEIA/LiPA$_{25}$ (version 1) and HPVE6*I mRNA was analysed by RT-PCR. As control for DNA quality, in HPV DNA negative cases, PCR

for the tubulin gene was done. Immunohistochemistry for $p16^{INK4a}$, pRb, Cyclin D1 and p53 was performed. Available information of the cases included anatomical site/subsite, country, gender, age and year of diagnosis.
Results: Preliminary results are based on a series of 4109 HNC cases: 1398 from the oral cavity (OC), 1545 from the pharynx (OP), and 1166 from the larynx (Lx) were tested. HPV/DNA negative and tubulin negative cases (n=368) were excluded. Overall HPV/DNA detection was: 9.3% in OC, 27.6% in OPx, and 7.2% in Lx. Both mRNA and p16 positive results in addition to HPV/DNA were detected in 3.0% OC, 18.3% OPx and 1.6% Lx. HPV16 was the most common type among HPV positive HNC cases (76.6%). Statistical analyses showed significant regional differences in HPV/DNA detection (in all sites), as well as a higher prevalence in females (OP, Lx), in younger ages at diagnosis (OP, Lx), and in cases from recent years (OP). Regarding histology, most HPV/DNA positive cases were OC/OP non keratinizing squamous carcinoma, basaloid and mixed squamous carcinoma.
Conclusions: This large study on HPV in HNCs provides a thorough approach to evaluate the HPV role in these tumors. The HPV contribution will help to understand the natural history of these cancers and will be essential to assess the potential value of HPV vaccines for the prevention of these cancers.

1309 The Utility of MDM2 and CDK4 Staining in Head and Neck Osteosarcoma

Abberly Lott Limbach, Reza Mostofi, Mark Lingen, Nicole Cipriani. University of Chicago, Chicago, IL; Oral and Maxillofacial Pathology, Biopsy Service, Chicago, IL.
Background: Osteosarcoma of the head and neck is rare. It more frequently occurs in long bones, where MDM2 and CDK4 are useful in distinguishing low-grade osteosarcoma from other benign mimics. Given the rarity of osteosarcoma in the head and neck, few studies have looked at the utility of these stains in gnathic osteosarcoma. We aim to investigate the utility of MDM2 and CDK4 stains in head and neck osteosarcomas as a means of distinguishing them from benign fibro-osseous lesions.
Design: We searched the surgical pathology archives for cases of bone lesions in the head and neck. The slides were reviewed to confirm the diagnosis and to select blocks for staining. MDM2 and CDK4 stains were performed on a representative block from each case and were reviewed by two authors. MDM2 and CDK4 were considered positive if nuclear staining was seen in tumor cells.
Results: Cases included 11 osteosarcomas from 10 patients (9 males, 1 female) with an average age of 37 years (range 14-70 years). Anatomic locations included the mandible, maxilla, and skull. There were 16 benign cases (6 males, 10 females) with an average age of 37 years (range 6-86), including 6 fibrous dysplasia, 4 cemento-ossifying fibroma, 2 peripheral ossifying fibroma, and 4 central giant cell lesions. MDM2 and CDK4 stained rare tumor cells in 55% of malignant cases (see table 1). Of note, MDM2 nuclear staining was present in associated osteoclast-like giant cells of both benign and malignant cases.

Tumor (N)	MDM2 positive	MDM2 negative	CDK4 positive	CDK4 negative
Osteosarcoma (11)	6 (55%) (focal weak)	5 (45%)	1 (9%) (focal weak)	10 (91%)
Benign tumors (16)	0 (0%)	16 (100%)	0 (0%)	16 (100%)

Conclusions: MDM2 and CDK4 staining has been shown to be useful in differentiating low-grade osteosarcoma from benign mimics in long bones. We examined the utility of MDM2 and CDK4 in osteosarcomas of the head and neck and found that MDM2 and CDK4 were weakly and focally positive in 55% and 9% of cases, respectively. All benign tumors in our study were negative for both MDM2 and CDK4. MDM2 staining in nuclei of osteoclast-like giant cells in both benign and malignant cases represents a potential diagnostic pitfall. MDM2 and CDK4 staining, if present in tumor cells, can aid in a diagnosis of osteosarcoma, but due to focal weak staining in tumor cells in conjunction with positive staining in giant cells, caution should be exercised when interpreting positive stains. Conversely, a diagnosis of osteosarcoma should not be excluded if stains are negative.

1310 Comparison of Genomic Profiles Between Recurrent Pleomorphic Adenoma and Pleomorphic Adenoma

Fernanda Mariano, Rogerio Gondak, Erika Egal, Felipe Fidalgo, Alfio Tincani, Ricardo Coletta, Oslei de Almeida, Luiz Kowalski, Ana Krepischi, Albina Altemani. Faculty of Medicine - UNICAMP, Campinas, SP, Brazil; Faculty of Santa Catarina, Florianópolis, SC, Brazil; A.C.Camargo Cancer Center, São Paulo, Brazil; Piracicaba Dental School - UNICAMP, Piracicaba, SP, Brazil; Institute of Biosciences - USP, São Paulo, Brazil.
Background: The majority of pleomorphic adenoma (PA) shows karyotype abnormalities, of which rearrangements involving 8q12-15 are the most common. The recurrence of tumor can be caused either by increase in the complexity of genetic abnormalities or by acquisition of promoting mutations. As in recurrent pleomorphic adenoma (RPA) genetic alterations has yet to be investigated, the aim of this study was to assess by array comparative genomic hybridization (aCGH) the genomic profile of copy number alterations associated with RPA and PA.
Design: Four cases of RPA and thirteen cases of PA were evaluated by array-CGH using a 180K platform. Data was analyzed using Nexus Copy Number Discovery.
Results: The RPA group showed no copy number alteration, except for one case that exhibited losses in 5p15.33p15.1, 5q13.1q35.3 and 12q12q13.11. PA group also showed few copy number alterations, and the most frequent findings involved the chromosome 8: 8p21.3p12 (gain), 8q12.1 (loss), 8p23.3q24.3 (gain), and 8q12.1q21.11 (gain). Genomic amplifications were revealed in the PA group, and relevant affected genes were *MAML2* and *LIFR*.
Conclusions: PAs and RPAs exhibited different patterns of genomic profile. This result suggests that despite the common origin theses tumors, the trigger can be by different mechanisms of tumorigenesis. Copy number alterations at chromosome 8 and the amplification of *MAML2* and *LIFR* genes can be a contributory factor in PA tumorigenesis. However, these genetic alterations might not to play role in the tumor recurrence (FAPESP: 2011/23204-5, 2011/23366-5).

1311 Genomic Profile Associated With Progression in Salivary Duct Carcinoma Ex Pleomorphic Adenoma

Fernanda Mariano, Rogerio Gondak, Ricardo Coletta, Oslei de Almeida, Luiz Kowalski, Ana Krepischi, Albina Altemani. Faculty of Medicine - UNICAMP, Campinas, SP, Brazil; Faculty of Santa Catarina, Florianópolis, SC, Brazil; Piracicaba Dental School - UNICAMP, Piracicaba, SP, Brazil; A.C.Camargo Cancer Center, São Paulo, Brazil; Institute of Biosciences - USP, São Paulo, Brazil.
Background: Salivary duct carcinoma ex pleomorphic adenoma (SDCEPA) is the most common type of carcinoma arising from pleomorphic adenoma (PA). SDCEPA arises within the PA and progresses invading beyond its capsule. To the best of our knowledge, the genomic profile of SDCEPA during tumor progression has not been studied. The aim of this study was to investigate by array comparative genomic hybridization (aCGH) the copy number alterations associated with tumor progression in SDCEPA.
Design: Nine cases of SDCEPA were evaluated by array-CGH using a 180K platform. Data was analyzed using Nexus Copy Number Discovery.
Results: SDCEPA was classified as intracapsular (IC) – two cases, minimally invasive (MI)- two cases and frankly invasive (FI)- five cases. Both IC cases showed different copy number alterations involving the chromosomes: 5, 6, 8, 9, 10, 12, 14, 16, 17, 22. 8p23.3p11.23 loss was identified in both cases. Amplified genes as *MLLT6, LASP1, CDK12, ERBB2,* and *KDM5A* were found. One MI case showed 6q12q27 loss and 12p13.33q24.33 gain. FI cases presented the highest number of copy number alterations involving the chromosomes: 1, 2, 3, 6, 8, 9, 15, 17, 18. 1q21.1q44 gain and 6q12q27 loss were identified in 2/5 FI cases, in addition to *CDK12* and *ERBB2* amplifications.
Conclusions: Somatically acquired copy number alterations, mainly amplifications, can be important for the initial step of the carcinogenesis of SDCEPA. The chromosome 12 gain suggests its participation in this early stage of tumor progression. In advanced tumors, there is an increased number of copy number alterations, of which some could be linked to the aggressive phenotype, particularly 1q21.2q44 gain (FAPESP: 2011/23204-5, 2011/23366-5).

1312 Somatic Copy Number Alteration Associated With Malignant Transformation and Progression of Carcinoma Ex Pleomorphic Adenoma

Fernanda Mariano, Rogerio Gondak, Felipe Fidalgo, Antonio Martins, Ricardo Coletta, Oslei de Almeida, Luiz Kowalski, Ana Krepischi, Albina Altemani. Faculty of Medicine - UNICAMP, Campinas, SP, Brazil; Faculty of Santa Catarina, Florianópolis, SC, Brazil; A.C.Camargo Cancer Center, São Paulo, Brazil; Piracicaba Dental School - UNICAMP, Piracicaba, SP, Brazil; Institute of Biosciences - USP, São Paulo, Brazil.
Background: Several genetic alterations have been identified in carcinoma ex-pleomorphic adenoma (CXPA), particularly those that are involved in the malignant transformation of the pleomorphic adenoma (PA). As the different phases of the carcinogenesis can be found in CXPA, the aim of this study was to investigate the somatic copy number alterations and involved genes possibly associated with the different stages of the tumor progression.
Design: Twenty six cases of CXPA and thirteen cases of PA were evaluated by array-CGH using a 180K platform. Data were analyzed using Nexus Copy Number Discovery.
Results: The CXPA cases were classified as early invasive (8) and frankly invasive (18). The most relevant chromosomal alterations in each group were: chromosome 8 (PA), chromosome 8 and 12 (early invasive) and 1, 5, 6, 8 and 12 (frankly invasive). The amplified genes found in each group were: *MAML2* and *LIFR* (PA), *KDM5A, MLLT6, LASP1, CDK12, ERBB2* (early invasive) and *MAML2, BIRC3, CDK4, LRIG3, WIF1, HMGA2, MDM2, CDK12, ERBB2, LYL1, EGFR, WHSC1L1*, *FGFR1* (frankly invasive).
Conclusions: Tumor progression of CXPA seems to be associated with an increase of somatic copy number alterations during carcinogenesis. Alterations involving chromosome 8 seems to be important from PA tumorigenesis to frankly invasive carcinoma, whereas copy number alterations involving chromosome 12 appear to be acquired in early invasive carcinoma and maintained in frankly invasive carcinoma. Copy number alterations of chromosomes 1, 5 and 6 would be added in the late stage of the carcinogenesis. *KDM5A, MLLT6, LASP1, CDK12, ERBB2* genes may be associated with malignant transformation while *BIRC3, CDK4, LRIG3, WIF1, HMGA2, MDM2, LYL1, EGFR, WHSC1L1*, *FGFR1* would be related to malignant progression (FAPESP: 2011/23204-5, 2011/23366-5).

1313 Survey of SMO and BRAF Mutational Status in Head and Neck and Adnexal Neoplasms

Andrew McClary, Jewison Biscocho, Sushama Varma, Jonathan Pollack, Robert West. Stanford University, Stanford, CA.
Background: Recently, we published a report detailing recurrent Smoothened (SMO) and BRAF mutations in ameloblastoma (Nature Genetics, 2014, 46:722). Interestingly, our findings highlighted the relationship between ontogenesis and oncogenesis, in particular, with respect to the biology of epider-mal placodes, which are miniorgans that generate both teeth and hair. For example, patient's diagnosed with nevoid basal cell carcinoma syn-drome (or Gorlin syndrome), which is defined by germline inactivating PTCH1 mutations, develop keratocystic odontogenic tumors (KCOT) in addition to basal cell carcinomas. Although, KCOTs are distinct from ameloblastomas, they underscore the dual role of Hedgehog signaling in odontogenic and cutaneous neoplasms. Due to this relationship, and the discovery of BRAF mutations in ameloblastoma, we wanted to broaden our survey to additional head and neck and adnexal tumors.

Design: Sanger DNA sequencing for known recurrent mutations in oncogenes involved in the epidermal placode biology was performed on archival FFPE blocks from cases of ameloblastic carcinoma, odontogenic keratocyst, ameloblastic fibroodontoma, dentigerous cyst, basaloid squamous cell carcinoma, trichoblastoma, spiradenoma, eccrine poroma, pilar sheath acanthoma, and syringocystadenoma papilliferum.
Results: Thus far in our preliminary survey (n=19 cases spanning the above diagnoses), a single SMO L412F mutation was found in ameloblastic carcinoma (n=1, 100%), as well as a BRAF V600E in ameloblastic fibroodontoma (n=1, 100%). All other screened cases were negative for SMO L412F and BRAF V600E.
Conclusions: Our study represents the first to profile the genomic mutational landscape of several rare neoplastic entities, many of which are associated developmentally with the epidermal placode. Mutations were identified in both SMO and BRAF in two rare odonotogenic tumors, ameloblastic carcinoma and ameloblastic fibroodontoma, which continues to point toward the relationship between ontogenesis and oncogenesis. Further studies, both with increased genomic coverage and numbers of samples, will enable continued discoveries that increase our understanding of both development and neoplastic transformation.

1314 Adenosquamous Carcinoma of the Head and Neck: A Covariate-Adjusted Study Showing Worse Outcome Compared To Conventional Squamous Cell Carcinoma

Mitra Mehrad, Kathryn Trinkaus, James Lewis. Washington University School of Medicine, St. Louis, MO.
Background: Adenosquamous carcinoma (AdSC) is a distinct and rare, biphasic variant of squamous cell carcinoma (SCC) defined by the presence of both SCC and any amount of adenocarcinoma, which has punched out gland spaces and usually associated mucin production. It has been reported in some studies as being more aggressive than conventional SCC, but no case control study with SCC has been performed to date. It is also unknown whether the quantity of the adenocarcinoma component affects outcome.
Design: We conducted a retrospective, covariate adjusted study with 23 cases of AdSC (with at least 6 months of clinical follow up for surviving patients) and 1883 controls treated between 1999 and 2012. Results are adjusted for age, site, overall stage, smoking, and for oropharynx cases, p16 status. The adenocarcinoma component was quantified in AdSCs by high power fields (HPF) with gland formation as low (≤ 10 HPF), moderate (11-49 HPF) and high (≥ 50 HPF). Clinical follow-up data was obtained by chart review.
Results: The adjusted matched cohort for AdSC had a significantly greater risk of recurrence, death of any cause, and death of disease, with global p-values of <0.0001 for both disease free survival (DFS) and disease specific survival (DSS). The individual case vs. controls p-value for DFS and DSS were 0.0018 and 0.034, respectively [DFS hazard ratio (HR): 2.37 (95% CI: 1.38-4.07) and DSS HR: 2.10 (95%CI: 1.06-4.16)]. The quantity of adenocarcinoma did not correlate with disease recurrence or survival (p-values= 0.1).
Conclusions: This is the first covariate adjusted study on survival in AdSC compared to conventional SCC, and it showed that AdSC patients have poorer survival, even while controlling for p16 status in the oropharyngeal cases. It also suggests that the current WHO definition of AdSC, which does not require any minimum quantity of gland formation for the diagnosis, is a clinically accurate one.

1315 DNA Methylation Analysis By Bisulfite Next Generation Sequencing To Early Detect Oral Squamous Cell Carcinoma From Oral Scrapings

Luca Morandi, Sofia Asioli, Valentina Monti, Achille Tarsitano, Claudio Marchetti, Davide Gissi, Lucio Montebugnoli, Maria Pia Foschini. University of Bologna, Bologna, Italy.
Background: Oral squamous cell carcinoma (OSCC) is the most frequent neoplastic disease in head and neck region and it is commonly preceded by potentially malignant lesions. The discovery of highly sensitive and specific biomarkers to identify those lesions having a high risk to undergo malignant transformation is urgently required. Aim of the present study is to evaluate the methylation status of a list of candidate genes from oral scraping specimens to improve the current strategies for early cancer detection with non-invasive methods.
Design: Oral scraping from 11 OSCC, 9 High Grade Squamous intraepithelial Lesion (HG-SIL), 9 Low Grade SIL(LG-SIL), 9 oral lichen planus (OLP) and 8 healthy donors were included in this study. PAP smear evaluation was done to confirm the presence of lesional cells within the brush. DNA was purified and bisulfite treated. A set of previously described differentially methylated genes in OSCC (*GP1BB, ZAP70, KIF1A, p16[CDKN2A], CDH1, miR137, miR375*) were investigated by bisulfite-Next Generation Sequencing (GSJunior, Roche, Branford, CT). ReadSeqs in Fasta format were analyzed by QuMA (http://quma.cdb.riken.jp/). The statistical significance between lesions and normal epithelia from the same patient and from a pool of healthy donors were evaluated with the Mann-Whitney U-test. Additionally *TP53* mutation analysis for exon 4-9 were performed by the same NGS platform.
Results: *ZAP70* was found to be hypermethylated in 100% of OSCC and HG-SIL cases, in 28.5% of LG-SIL and in none of OLP. *GP1BB* hypomethylation was detected in 90.9% OSCC, in 88.8% of HG-SIL, 37.5% of LG-SIL and in none of OLP. *MIR137* was hypermethylated in 100% of OLP, while only in 44.4% of OSCC, 50% in HG-SIL, 25% in LG-SIL. Hypermethylation in proximal promoter of *KIF1A* was detected in 54.5% OSCC, 33.3% HG-SIL, 50% LG-SIL and 0% in OLP. No epigenetic aberrations were detected in normal healthy donors. *p16, CDH1* and miR375 did not revealed variations in the methylation pattern for all the classes.
Conclusions: In our preliminary results, Bisulfite-NGS analysis of *GP1BB, ZAP70* and *miR137* promoters from oral scrapings allows to discriminate OSCC and HG-SIL from LG-SIL, OLP and normal oral mucosa. HG-SILs share the same epigenetic modifications of OSCC. These data confirm that CpG methylation changes may play a role in oral cancer progression and that DNA methylation analysis may have significant utility in early detection of OSCC. Furthermore the method here proposed is non invasive and can be applied to screen patients.

1316 PRKD Gene Family Somatic Alterations in Polymorphous Low-Grade Adenocarcinomas of the Salivary Glands

Salvatore Piscuoglio, Ilan Weinreb, Luciano Martelotto, Charlotte Ng, Nicola Fusco, Brian Rubin, Britta Weigelt, Jorge Reis-Filho. Memorial Sloan Kettering Cancer Center, New York, NY; University Health Network, Toronto, ON, Canada; Cleveland Clinic, Cleveland, OH.
Background: Polymorphous low-grade adenocarcinoma (PLGA) is the second most common intra-oral salivary gland malignancy. We have recently identified a E710D hotspot activating mutation in the *PRKD1* serine/threonine kinase in 73% of PLGAs, which likely constitutes a driver event. Other PRKD gene family rearrangements have been identified in cribriform adenocarcinoma, a salivary gland tumor closely related to PLGAs. Given that PRKD2 and PRKD3 share similar functions and kinase domain sequence with PRKD1, we hypothesized that *PRKD1* wild-type PLGAs might harbor somatic genetic alterations in *PRKD2* or *PRKD3*.
Design: Seventeen PLGAs with wild-type *PRKD1* status (1 frozen and 16 FFPE) were retrieved from the pathology files of Memorial Sloan Kettering Cancer Center and University Health Network. All cases were reviewed by two pathologists. DNA and RNA were extracted from microdissected tumor tissue. RNA from one *PRKD1* wild-type PLGA was subjected to paired-end RNA-sequencing. Fusion genes were identified by ChimeraScan and deFuse algorithms; annotation and prediction was performed using Oncofuse. DNA samples from the 17 wild-type *PRKD1* PLGAs were subjected to Sanger sequencing with primers for the exons coding for the kinase domain of *PRKD2* and *PRKD3* genes.
Results: Sequencing analysis of 17 *PRKD1* wild-type PLGAs demonstrated that the kinase domain of *PRKD2* and *PRKD3* genes had wild-type sequences in all cases. RNA-sequencing analysis of one *PRKD1* wild-type PLGA revealed an in-frame *ACTN4-PRKD2* fusion gene, which was considered high confidence by ChimeraScan and DeFuse, and was validated by RT-PCR. This fusion gene was found to be potentially pathogenic by Oncofuse, and comprises exons 12 to 19 of *PRKD2* and 1 to 8 of *ACTN4*. The predicted ACTN4-PRKD2 fusion protein contains the intact kinase domain of PRKD2. Expression of the fusion gene is under the control of the *ACTN4* promoter, which is highly expressed in salivary gland tissues. Of the additional 8 *PRKD1* wild-type PLGAs tested by RT-PCR, none harbored the *ACTN4-PRKD2* fusion gene.
Conclusions: The kinase domains of *PRKD2* and *PRKD3* are not targeted by somatic mutations in *PRKD1* wild-type PLGAs. One *PRKD1* wild-type PLGA harboured an *ACTN4-PRKD2* gene fusion. Further studies are warranted to define other driver genetic events in *PRKD1* wild-type PLGAs.

1317 Transcriptionally Active Human Papillomavirus Is Detected By RNA In Situ Hybridization in Most Discordant Oropharyngeal Squamous Cell Carcinomas That Are P16 Positive By Immunohistochemistry But High Risk HPV Negative By DNA In Situ Hybridization

Lisa Rooper, Peter Illei, Justin Bishop, William Westra. Johns Hopkins Hospital, Baltimore, MD.
Background: Confirmation of HPV status in oropharyngeal squamous cell carcinoma (OPSCC) has become increasingly important for prognostication, enrollment in clinical trials, and consideration of therapeutic de-escalation. Despite these compelling clinical needs, HPV status is ambiguous in those OPSCCs that are p16 positive by immunohistochemistry (IHC) but HPV negative by DNA in situ hybridization (DISH). It is not clear whether these discordant cases reflect: 1) induced p16INK4a expression through non-viral mechanisms, or 2) suboptimal sensitivity of DISH platforms. Recently, E6/E7 mRNA ISH (mRISH) has become available for identification of transcriptionally active high risk HPV in formalin fixed, paraffin embedded tissues. Application of this next generation HPV detection assay to p16-positive/DISH-negative cases could help explain HPV discordance and provide more certainty regarding HPV status.
Design: The surgical pathology files of the Johns Hopkins Hospital were reviewed for cases of OPSCC that were p16 positive by IHC, but high risk HPV negative by DISH using the Ventana Inform HPV III Family 16 Probe system. Of the 28 cases identified, 21 were selected for mRISH using RNAscope HPV kit for detection of high risk types 16, 18, 26, 31, 33, 35, 39, 45, 51, 52, 53, 56, 58, 59, 66, 68, 73 and 82. The mRISH results were independently scored by 3 pathologists (PBI, JAB, and WHW) and 1 pathology resident (LMR).
Results: Transcriptionally active E6/E7 mRNA was identified in 20 of 21 (95%) cases. Positive cases were identified as multiple dot-like hybridization signals that were restricted to the nuclei of tumor cells. In 3 cases the hybridization signals could only be identified at 20X magnification, and in 17 cases the signals were intense, abundant and easily visualized at 10X magnification. There was 100% agreement in scoring these cases as positive or negative among all 4 observers.
Conclusions: For OPSCCs, the vast majority of p16-positive/DISH-negative discordant cases are due to the insensitivity of current DISH platforms. The next generation mRISH platform is sensitive, provides direct evidence of viral transcriptional activity, is transferrable to the surgical pathology laboratory, and is easy to interpret. E6/E7 mRISH should be considered as a first-line platform for determination of HPV status of OPSCCs.

1318 Predictive Factors and Topography of Nodal Metastases From Oral Cavity Squamous Cell Carcinoma – an Audit of 304 Cases Undergoing Primary Surgical Resection

Paromita Roy, Sonali Nayak, Indu Arun, Divya Midha, Arun Pattatheyil, Kapila Manikantan, Sanjoy Chatterjee, Indranil Mallick. Tata Medical Center, Kolkata, India.

Background: Nodal metastasis(NM) is an important prognostic factor in oral cavity squamous cell carcinoma(OSCC). Prevalence and distribution of NM plays a key role in determining extent of surgery and subsequent radiotherapy.

Design: We retrospectively analyzed the pathology records of 304 patients with OSCC (Sep2011-May2014), undergoing primay surgical resection, to determine the predictors and level-wise pattern of NM and extracapsular extension(ECE). Chi-square test and binary logistic regression was used to analyze predictive factors.

Results: There were 247 (81%) unilateral and 57 (19%) bilateral neck dissections. Majority (82%) required level IV dissection. 12,615 nodes were examined (median 37/case). Pathological stage was pN0, pN1, pN2a, pN2b, pN2c and pN3 in 59%, 15%, 1%, 21%, 3%, 1% respectively.

Predictors of NM included age <50 yrs (48% vs 37%, p=0.045), grade (well, moderate, poor =10%, 44%, 52% p<0.001), T3/T4 primaries (52% vs. 35%, p=0.004), tumour size (<2cm, > 2 cm = 20% vs. 48%, p<0.001), lymphovascular invasion (LVI) (84% vs 10%, p<0.001), perineural invasion (PNI) (61% vs. 24%, p<0.001), depth of infiltration (0-5mm, 6-10mm, >10mm = 9%, 41%, 56% p<0.001). There was no difference in the incidence of nodal metastases between primary sites of oral tongue, buccal mucosa, gingiva and retromolar trigone (43%, 42%, 39% and 44% respectively). LVI and PNI were independent predictors on multivariate analysis.

Topographical analysis revealed NM to levels IIb, IV and V was uncommon

	Ipsilateral neck nodes		Contralateral neck nodes
Level	Incidence (all patients)	Incidence (node positive cases)	Incidence (node positive cases)
Ia	5.3%	12.7%	
Ib	25.7%	61.9%	4.8%
IIa	22.7%	54.8%	27%
IIb	2.0%	4.8%	0%
III	8.2%	19.8%	0%
IV	2.6%	6.4%	0%
V	1.6%	4.0%	0%
Perifacial	2.3%	5.6%	

Skip metastasis to levels III and IV was present in 7(5.5%) patients, all with oral tongue primaries.

ECE was seen in 65 patients (51% of N+ patients), and was nonsignificantly higher for buccal versus oral tongue primaries (63% vs. 47%, p=0.11).

Conclusions: Several factors especially LVI and PNI predict for NM. Metastases to the lower and posterior neck is uncommon. Further studies could investigate the role of customizing neck treatment based on predictive and topographical factors.

1319 Role of SOX10 in the Differential Diagnosis of Oncocytic Salivary Gland Neoplasms

Alessandra Schmitt, Ifeoma Nwadei, Cynthia Cohen, Momin Siddiqui. Emory University, Atlanta, GA.

Background: Numerous salivary gland neoplasms show oncocytic features, including acinic cell carcinoma (AciCC), Warthin tumor (WT), mucoepidermoid carcinoma (MEC), and oncocytoma (ONC). We investigated the role of SOX10 in separating these oncocytic salivary gland neoplasms on fine needle aspiration (FNA) cell blocks (CB) and on resections. A comparison with DOG1, p63, and S100 immunohistochemical (IHC) stains was also performed.

Design: 31 FNA CB of oncocytic salivary gland neoplasms (10 AciCC, 16 WT, 3 MEC, 2 ONC), and 74 salivary gland resections (26 AciCC, 7 WT, 36 MEC, 2ONC, 2 high grade adenocarcinomas [ADC], and 1 papillary cystadenoma [PC]} were stained for SOX10, DOG1, p63, and S100.

Results: IHC results of CB [Table 1] and resections [Table 2]. SOX10 (nuclear) [Figure 1] and DOG1 (membranous) [Figure 2] staining of AciCC.

Table 1

N=31	SOX10	DOG1	p63	S100
AciCC (10)	5 (50%)	7 (70%)	0	0
WT (16)	0	0	14 (87.5%)	0
MEC (3)	0	0	3 (100%)	0
ONC (2)	0	0	1 (50%)	0

Table 2

N= 74	SOX10	DOG1	p63	S100
AciCC (26)	25 (96%)	24 (92%)	3 (11.5%)	2 (8%)
WT (7)	0	0	6 (86%)	0
MEC (36)	4 (11%)	19 (53%)	35 (97%)	0
ONC (2)	0	0	2 (100%)	0
ADC (2)	1 (50%)	0	1 (50%)	0
PC (1)	0	1 (100%)	1 (100%)	0

Figure 1

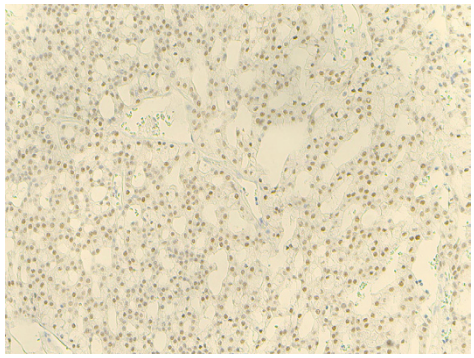

Figure 2

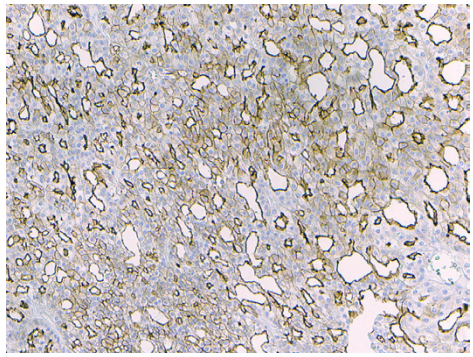

Conclusions: SOX10, DOG1, and p63 are helpful to distinguish AciCC from WT in CBs, since 100% of WT were SOX10- and DOG1- and 87.5% were p63+, whereas 50% and 70% of AciCC were SOX10+ and DOG1+ respectively and 100% of AciCC were p63-. The resection results correlated with those of CBs: 100% of WT were SOX10- and DOG1- and 86% were p63+, whereas 96% and 92% of AciCC were SOX10+ and DOG1+ respectively, and 88.5% were p63-. Less than 10% of resected AciCC were S100+. In summary, these markers were useful in distinguishing AciCC from other oncocytic neoplasms.

1320 Clinicopathologic and Molecular Characterization of High Grade Polymorphous/Cribriform Adenocarcinomas of Salivary Gland

Raja Seethala, Isabel Fonseca, Cristina Antonescu, Bayardo Perez-Ordonez, Ilan Weinreb. University of Pittsburgh, Pittsburgh, PA; Instituto Português de Oncologia, Lisbon, Portugal; Memorial Sloan Kettering Cancer Center, New York, NY; University Health Network, Toronto, Canada.

Background: Polymorphous low grade adenocarcinoma (PLGA) and cribriform adenocarcinoma of salivary gland (CASG) are classically considered low grade tumors with occasional late locoregional recurrence, the latter entity being more aggressive. Higher grade versions of these tumors are rare and not well characterized. We describe the clinical and morphologic characteristics as well as *PRKD1-3* gene rearrangement status of five cases of high grade polymorphous/cribriform adenocarcinomas (HGPCA).

Design: Five cases were included based on the presence of: 1) growth patterns of either PLGA (targetoid fascicular), CASG (glomerulopapillary), or both (mixed); 2) Nuclear and chromatin characteristics of PLGA and/or CASG but with nuclear anisomorphism (size variation ≥ 4:1); and 3) ≥ 5 mitoses per 10 high power fields (HPF). Immunohistochemical stains for S100, p63, and either smooth muscle actin or calponin were performed on all cases. Fluorescence in situ hybridization for *PRKD1-3*, *ARID1A*, and *DDX3X* was performed using previously characterized breakapart probes (CHORI; Oakland, CA).

Results: Clinicopathologic features and gene rearrangement status are summarized in table 1. All HGPCA were S100 positive and smooth muscle actin/calponin negative. P63, when positive, was focal and weak.

Case	Gender	Age (yrs)	Site	Size (cm)	Neck Disease	Predominant Growth Pattern	Solid Overgrowth	Necrosis	Gene Rearrangement	Follow up
1	M	82	Upper Lip	3.8	---	Mixed	Yes	Yes	No	Local recurrence at 28 months
2	F	59	Mandible	6.9	Yes	CASG (rhabdoid)	No	No	ARID1A, PRKD1	Cervical spinal metastasis at 26 months
3	F	55	Retromolar trigone (recurrence)	4	Yes	CASG	Yes	Yes	PRKD3	Current case is locoregional recurrence at 54 months
4	F	66	Hard Palate	3.2	---	Mixed	Yes	Yes	No	No disease 12 months
5	M	36	Hard Palate	7	---	CASG	Yes	Yes	PRKD3	No disease 26 months

Conclusions: Morphologic, immunophenotypic and molecular features appear to support HGPCA as a rare form of tumor progression in PLGA and CASG. Solid overgrowth and necrosis are common features. Translocation positive cases have a CASG predominant growth pattern similar to their well differentiated counterparts. When HGPCA recur, they do so fairly quickly in keeping with a more aggressive phenotype.

1321 Association of Cell Signalling Factors With Survival and Anti-EGFR (Cetuximab) Resistance in Head and Neck Squamous Cell Carcinoma

Maria Eugenia Semidey-Raven, Margarita Alberola-Ferranti, Jordi Giralt, Javier Hernandez-Losa, Victor Rodriguez-Freixinos, Sergio Benavente, Teresa Moline, Santiago Ramon y Cajal. Vall d´Hebron University Hospital, Barcelona, Spain.

Background: Head and neck squamous cell carcinoma (HNSCC) has one of the highest mortality rates in malignant pathology. Cetuximab has long been approved for treating locally advanced disease, demonstrating benefits in prolonged locoregional control, progression-free survival and overall survival. Nevertheless, resistance mechanisms that arrest its effectiveness have emerged. We analyzed the expression of cell signalling factors in HNSCC that may have a leading role in resistance mechanisms.

Design: This was a retrospective and observational study including patients with diagnosis of HNSCC. Patients were classified according to TNM classification. Immunohistochemistry for pMAPK, pmTOR, pS6, 4E-BP1, p4EBP1, eIF4E, peIF4E, PTEN, Ki67 and p16 was performed. Expression levels were semiquantitatively evaluated as percentage and intensity of stained tumor cells [H-score]. Survival and time to recurrence for each signal factor were evaluated by Kaplan Meier analysis and compared by log rank tests.

Results: We included 90 patients with HNSCC. According to TNM classification, there were 19 (21,2%) patients with stage T1-T2, 71 (78,8%) with T3-T4, 25 (27,8%) with N0, and 65 (72,2%) with N+. We found a significant lower time to death in those patients with tumors expressing pMAPK (*H-score* >40, log rank p=0,008) and a tendency in the time to recurrence (log rank p=0,058). In addition, a lower time to recurrence was observed in patients with tumors expressing pmTOR (*H-score* >20, log rank p=0,01) and no expression of p16 (*score* <20, log rank p=0,049). No other significant associations were observed.

Conclusions: The expressions of pMAPK and pmTOR were predictive factors of worse prognosis showing lower survival and time to recurrence. By contrast, the expression of p16 was associated to better survival and higher time to recurrence. Our findings suggest that expressions of pMAPK and pmTOR may have an independent activation mechanism despite Cetuximab blockage, causing a resistance to its effect. Therapy strategies combining anti-pmTOR/pMAPK inhibitors plus Cetuximab could be useful for treatment of patients with HNSCC.

1322 Carbonic Anhydrase IX in Sinonasal Renal Cell-Like Adenocarcinomas (SNRCLA) and Human Sinonasal Mucosa

Tiansheng Shen, Shuting Bai, Shi Wei, Margaret Brandwein-Gensler. University of Alabama, Birmingham, AL; New York University Medical Center, New York, NY.

Background: SNRCLA is a rare, enigmatic tumor resembling clear cell renal cell carcinoma (CCRCC). Its unique histology raises questions about origin, for SNRCLA bears no resemblance to sinonasal neoplasia derived from mucosa, minor salivary glands, or seromucinous glands. As SNRCLA resembles CCRCC, could this tumor be derived from endogenous "renal like" sinonasal tissue? Phylogenetically, birds and reptiles have nasal "salt glands" which act as "auxiliary kidneys" regulating ion concentration; they also express carbonic anhydrase IX (CA IX), typically expressed in CCRCC. It is known that SNRCLA do not express RCC, a renal cell carcinoma marker. Here, we investigate CA IX in SNRCLA and test the hypothesis that CA IX-expressing cells are present in human sinonasal tissue.

Design: CA IX expression was examined in 5 normal nasal specimens and 5 SNRCLA (mouse monoclonal antibody, Cell Marque, Rocklin, CA). CCRCC were used as positive control.

Results: CA IX expression was detected in all 5 sinonasal specimens. Patchy cytoplasmic and membranous CA IX expression was demonstrated in respiratory epithelial cells and submucosal glands (Fig 1). Three SNRCLA demonstrated strong, diffuse, cytoplasmic and membranous CA IX expression (Fig 2). One SNRCLA was CA IX negative, and the last one was technically noncontributory.

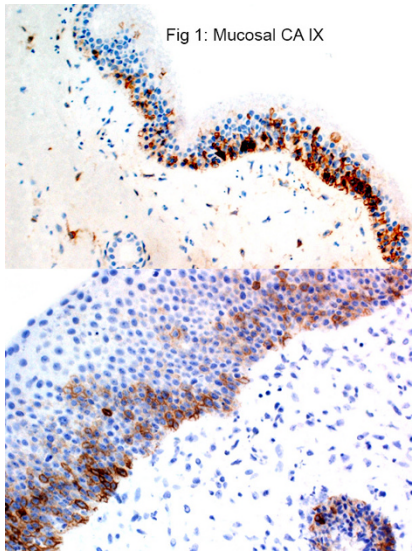

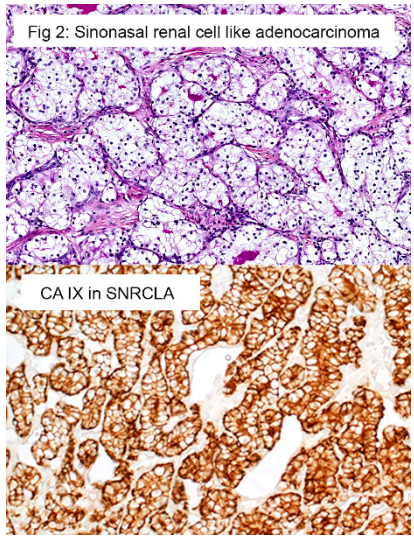

Conclusions: CA IX is commonly expressed in SNRCLA. This may be a useful biomarker for diagnostic confirmation. We demonstrate CA IX expression in normal sinonasal tissue. This is interesting as by comparison, CA IX is over-expressed in CCRCC, but not expressed in normal renal tissue. Additional studies are ongoing, including more sinonasal samples, CA II, and HIF-1. The data support the concept of endogenous sinonasal renal-like tissue which can regulate ion concentration. This may explain the origin of this rare sinonasal renal-like neoplasm.

1323 Utility of Microtubule-Associated Protein-2 (MAP2) Immunostain in Distinguishing Olfactory Neuroblastoma and Head and Neck Paraganglioma

Alexander Shtabsky, Leonor Leider-Trejo, Faina Misonzhnik-Bedny, Irit Solar. Tel Aviv Sourasky Medical Center, Tel Aviv, Israel; Tel Aviv University, Tel Aviv, Israel.

Background: Olfactory neuroblastoma (ON) and head and neck paraganglioma (PG) are neoplasms of different histogenesis but similar immunophenotype. The differential diagnosis is based on tumor morphology and clinical data however in some cases the distinction is difficult or even impossible. Expression of MAP2 has been described in neural, neuroendocrine and neural crest-derived neoplasms including PG. In contrast, description of MAP2 in human ON is limited to few case reports. This study aims to evaluate the utility of MAP2 in the differential diagnosis between ON and PG.

Design: Immunohistochemical stain for MAP2 was performed on 20 ON and six PG surgical cases. The intensity of the stain was semi-quantitatively evaluated as 0 (negative), 1+ (faint in 1-50% of cells or intense in 1-10%), 2+ (faint in 50-100% or intense in 10-50%), 3+ (intense in 50-100%).

Results: ON included 14 primary, four recurrent and two cases with both primary and recurrent/metastatic tumor. ON showed negative stain (0) in 75% of cases (15/20); 1+ stain in 10% (2/20); 0 or 1+ in 10% (2/20, with slight difference between primary and recurrent/metastatic tumor in the same patient); 2+ in 0% (0/20); 3+ in 5% (1/20). Overall, 95% of ONs demonstrated either negative (0) or focal (+1) stain. In contrast, PG demonstrated intense diffuse stain (+3) in 100% of cases (6/6).

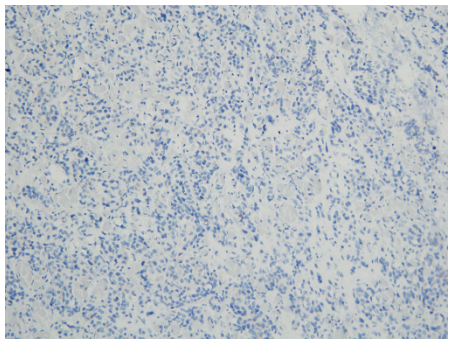

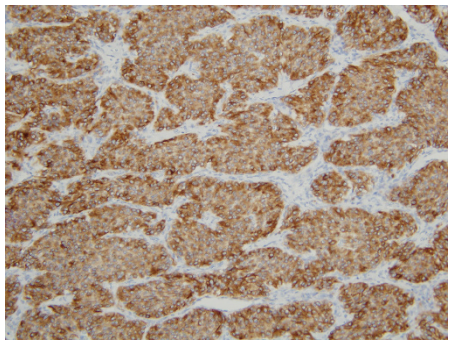

Diagnosis	Cases #	MAP2 Immunoreactivity				
		0	0 or 1+	1+	2+	3+
Olfactory neuroblastoma	20	15	2	2	0	1
Paraganglioma	6	0	0	0	0	6

Conclusions: Our results demonstrate that MAP2 is a reliable marker in differential diagnosis between ON and head and neck PG. MAP2 is strongly diffusely positive in PG and negative or focally weakly positive in majority of ONs. Strong focal/diffuse MAP2 stain in a small percentage of ONs could be in part explained by ganglioneuroblastic differentiation.

1324 Histological Risk Model Is a Useful and Inexpensive Tool To Assess Risk of Recurrence and Death in Stage I or II Squamous Cell Carcinoma of Oral Tongue

Namita Sinha, Matthew Rigby, Michael McNeil, Fawaz Makki, S Mark Taylor, Robert Hart, Jonathan Trites, Martin Bullock. QEII Health Sciences Center, Dalhousie University, Halifax, NS, Canada; IWK, Dalhousie University, Halifax, NS, Canada.

Background: Surgery is the mainstay of treatment for low stage (stage I/II i.e. T1N0/T2N0) squamous cell carcinoma of oral tongue (SCCOT). Adjuvant therapy is indicated in patients with higher stage SCCOT or with adverse prognostic factors. However, a significant percentage of low stage SCCOT will develop local recurrence and disease-related mortality. We used the existing Histological Risk Model (HRM) to assess 3 features (perineural invasion (PNI), lymphocytic host response (LHR), worst pattern of invasion (WPOI)) and classified the patients in three risk categories (RC- low (L), intermediate (I) and high (H)). We correlated RC and other variables with recurrence and death related to recurrence.

Design: We studied all patients (n=64) with stage I/II SCCOT who received surgical treatment between January 2001 and December 2013. The HRM was applied. Recurrence and mortality due to recurrence were determined. Univariate association between these outcomes and factors were tested using a 2-tailed Fisher exact tests. In addition, a multivariate analysis was performed using a logistic regression model to assess the association of recurrence with T-stage (1 vs. 2), margin status and RC (L/I vs. H).

Results: In a univariate model high RC tumors had a significantly higher rate of recurrence and death due to recurrence compared to low/intermediate RC-L/I (p=0.004 and p<0.001 respectively). Controlling for margin status and T stage, RC- H had a 2.43 odds ratio of later recurrence when compared with RC- L/I. This association was at a p value of 0.017. In addition, tumor thickness of 0.4 cm was significantly (p=0.026) associated with later recurrence, but not with death due to recurrence.

Conclusions: For stage I or II SCCOT, when compared to patients in the low or intermediate RC, patients in the high RC have a significantly higher risk for recurrence even when controlling for margin status and T-stage. These patients may be suitable candidates for adjuvant treatment to decrease morbidity and mortality associated with a recurrence. Our results indicate that the HRM is a useful tool to assess risk of recurrence in stage I or II SCCOT.

1325 Reactive Ganglioneural Proliferations of the Head and Neck Mucosae

Norbert Sule, Yunguang Liu, Richard Cheney, Mihai Merzianu. Roswell Park Cancer Institute, Buffalo, NY.

Background: Neural neoplasms of head and neck mucosa surface (HNMS) such as neurofibroma (NF) or ganglioneuroma (GN) are extremely rare and may harbinger a severe underlying condition (e.g., NF1 or MEN2B syndromes). Subepithelial nerve plexus (SNP) is a well described structure associated with lingual taste buds. Both hyperplastic SNP (HSNP) and traumatic neuroma (TN) or TN-like lesions (TNL) can mimic GN or NF. We review here these HNMS reactive (ganglio)neural proliferations (RGNP).

Design: Our database was searched for key words: neuroma, NF, GN; cases were reviewed and clinicopathologic findings summarized.

Results: Fifteen RGNP from 12 patients, 6 men and 6 women, mean age 66 (range, 46-88) years were seen in 13 biopsies and 2 excisions; 9 patients were treated, evaluated or followed for other tumors (4 HNSCC, 2 lymphoma, 1 papilloma, 1 salivary gland carcinoma, 1 prostate carcinoma) and only 3 presented with local signs/symptoms (base of tongue (BOT) firmness, leukoplakia, tongue "lesion").

Clinical exam found RGNP in 7 patients but in 5 they were incidental microscopic findings: 10 in BOT, 4 in oral tongue and one in larynx. RGNP were small (mean, 2.3; range, 0.5-5 mm), ill-defined (9 of 15), circumscribed (4 of 15) or diffuse (2 of 15); in 3 patients they were seen in different biopsies and in 3 BOT sites multiple HSNP were seen.

Histologic features of RGNP were variable resembling NF or TN in cases without ganglion cells and GN in HSPN. All lesions were superficial and non-encapsulated. Fibrosis was focal in 9, extensive in 4 and absent in 2; myxoid changes were seen in 3 of 15 RGNP. Taste buds were seen in 8 BOT and 1 oral tongue cases and absent in the rest; ganglion cells were seen in 8 of 15; 7 RGNP had both.

Associated pathologic findings were squamous hyperplasia (40%), squamous dysplasia (20%) and primary tumor (25%).

Original diagnoses were: GN (27%), TN (27%), RGNP (20%), neuroma (12%), NF (7%) and not specified (7%). IHC was used in 80% of cases diagnosed as neoplastic and only in 44% of those interpreted as reactive. After review, all lesions were reclassified as RGNP: 11 HSNP and 4 TNL. No patient had features of NF1 or MEN2B syndrome.

Conclusions: RGNP are superficial, occur in older patients subdjacent to lingual papillae (HSPN) and are commonly (34%) misinterpreted as neoplastic when ganglion cells are seen and ancillary studies are used. The term 'neuroma' should be avoided. Pathologists' awareness of normal histology and RGNP spectrum is key to avoid misclassification as NF or GN which, especially when multifocal, may trigger additional workup or unnecessary procedures.

1326 E-Cadherin and Twist 1 Expression in Salivary Gland Basal Cell Adenomas and Basal Cell Adenocarcinomas

Brennan Tesdahl, Thomas Wilson, Thomas Czeczok, Henry Hoffman, Robert Robinson. University of Iowa, Iowa City, IA.

Background: Basalcell adenoma (BCA) and basal cell adenocarcinoma (BCAC) represent uncommon basaloid salivary gland neoplasms that show marked morphologic similarity. Histologically they are primarily separated on the basis of invasion (BCAC) or lack of invasion (BCA) of the surrounding tissue. Epithelial-mesenchymal transition (EMT) is a process in which epithelial cells acquire invasive properties and metastatic potential in part by loss of adherence and their tight junctions. One of the mechanisms by which this happens is a decrease in the cell to cell adhesion molecule E-cadherin. A variety of transcription factors that are implicated in EMT, including Twist, which can repress E-cadherin through direct or indirect means. We wished to determine if specific proteins associated with EMT would be correlated to the presence or absence of invasion in these tumors.

Design: 30 BCA's and 19 BCAC's were identified. Tissue microarrays were constructed from paraffin blocks and stained using immunohistochemistry for E-cadherin and Twist 1. Scoring consisted of evaluating the staining on triple replicates of tissue cores. For E-cadherin cytoplasmic staining was determined to be positive or negative. For Twist 1, nuclear and cytoplasmic staining was assessed separately and semi-quantitated as to intensity of staining on a 0-3 score. Only tumors with a score of 2 or greater were considered positive. The location of the staining was noted to be either abluminal or luminal in the tumor cell nests for both antibodies.

Results: E-cadherin was expressed more frequently in the BCAC's than in the BCA's. (p = < .02). E-cadherin was seen to be preferentially expressed in the inner (luminal) layer of both tumor types as opposed to the abluminal cells. Twist 1 was seen to be nearly equally expressed in BCA's and BCAC's. Similarly to E-cadherin, staining was nearly always confined to the luminal layer of cells.

Conclusions: Both E-cadherin and Twist 1 expression appears to be more prominent in the luminal aspect of both BCA and BCAC's. Unexpectedly, E-cadherin was more frequently expressed in the BCAC's compared to the BCA's. No direct correlation was seen between expression of E-cadherin and Twist 1. If E-cadherin and Twist are involved in the presence or absence of invasion in these neoplasms, it appears that luminal type cells are preferentially involved over the abluminal cells.

1327 HPV-Related Large Cell Neuroendocrine Carcinoma of the Head and Neck

Elizabeth Thompson, Edward Stelow, Stacey Mills, William Westra, Justin Bishop. Johns Hopkins, Baltimore, MD; University of Virginia, Charlottesville, VA.

Background: A subset of oropharyngeal and sinonasal cancers is HPV-related. While most of these HPV-related cancers exhibit non-keratinizing squamous morphology, increasing experience has uncovered numerous histologic variants including tumors with basaloid, papillary and glandular features. HPV-related H&N cancer generally

has a good prognosis, but one variant - HPV-related small cell carcinoma (SmCC)- is important to recognize because it exhibits very aggressive behavior. We sought to characterize a previously unreported form of H&N cancer, HPV-related large cell neuroendocrine carcinoma (HPV-LCNEC).

Design: The authors' consultation files were searched for cases of HPV-LCNEC. Tumors were regarded as HPV-related if immunoreactive for p16 and positive by in situ hybridization for high risk HPV. The slides were reviewed, and the histologic and immunophenotypic features were described. In addition, pertinent clinical information was obtained from patients' medical records.

Results: Three cases of HPV-LCNEC were identified; they arose in 2 men and 1 woman, aged 57, 58, and 65. Two LCNECs were tonsillar and 1 arose in the sinonasal tract. Morphologically, the tumors consisted of nests and trabeculae of medium-large cells with abundant cytoplasm, vesicular chromatin and prominent nucleoli. Peripheral nuclear palisading, vague rosettes, very high mitotic rates and frequent areas of necrosis were noted. None exhibited squamous differentiation, but one tumor had a minor SmCC component. All cases were positive for pan-CK and synaptophysin. In contrast, all cases were p63-negative and only 1 was positive for CK5/6. Both tonsillar LCNECs had widely metastasized at the time of presentation, and the sinonasal LCNEC presented with skull base destruction and intracranial extension. One patient died of disease 3 months following presentation; outcome data for the others is forthcoming.

Conclusions: LCNEC is a rare form of HPV-related H&N cancer. The morphology of HPV-LCNEC overlaps considerably with the non-keratinizing appearance of HPV-related squamous cell carcinoma. As a result, HPV-related LCNEC may be underrecognized, and a high index of suspicion is needed to identify it. Abundant necrosis, very high mitotic activity, and neuroendocrine features like nuclear palisading or rosettes in a non-small cell HPV-related cancer are important histologic clues. Immunostaining for synaptophysin with absent p63 expression is confirmatory. Based on very limited data, HPV-LCNEC may be an aggressive variant similar to HPV-related SmCC. Additional cases and follow up information are needed.

1328 Parotid Gland Nodular Fasciitis: A Clinicopathologic Series of 12 Cases With a Review of 18 Cases From the Literature

Lester Thompson, Tyler Gibson, Justin Bishop. Southern California Permanente Medical Group, Woodland Hills, CA; Johns Hopkins Medical Institutions, Baltimore, MD.

Background: Nodular fasciitis (NF), very uncommon in the parotid gland, is a benign myofibroblastic proliferation that may be mistaken for other neoplastic proliferations. The mass-like clinical presentation and histologic features result in frequent misclassification, resulting in inappropriate clinical management. There are only a few reported cases in the English literature.

Design: Cases within the files of the authors' institutions (retrospective) confined to the parotid gland were compared to cases reported in the English literature (Medline 1966-2014).

Results: The patients included 5 females and 7 males, aged 11—70 years (mean 45.2 years). All patients presented with a mass lesion, present on average 1.9 months, without a documented history of trauma. The lesions were 0.7—5.2 cm (mean 2.2 cm). Seven patients had fine needle aspiration. The majority of the lesions were circumscribed (n = 9), composed of spindle-shaped to stellate myofibroblasts (MF) arranged in a storiform growth pattern, juxtaposed to hypocellular myxoid tissue-culture-like areas with extravasation of erythrocytes. Dense, keloid-like collagen (n = 7) and occasional giant cells were seen (n = 6). Mitotic figures (without atypical forms) were readily identifiable (mean 4/10 HPFs). By immunohistochemical staining, the MF were reactive with vimentin, actins, calponin, and CD68. All patients had surgical excision. One patient developed local recurrence (12 months later). All were alive and disease free at last follow-up, with a mean 133 months of follow-up. The principle differential diagnoses include fibrosarcoma, fibromatosis, pleomorphic adenoma, myoepithelioma, neurofibroma, schwannoma, solitary fibrous tumor, leiomyoma, fibrous histiocytoma and myxoma.

Conclusions: NF of the parotid gland occurs in middle-aged patients who present with a mass (mean 2.2 cm) in the parotid gland of short duration (1.9 months). FNA interpretation frequently leads to excision. Separation from myoepithelial and mesenchymal lesions affecting the parotid gland results in appropriate management.

1329 Sinonasal Tract Neurofibroma: A Clinicopathologic Series of 12 Cases With a Review of the Literature

Lester Thompson, Justin Bishop, Ari Azani. Southern California Permanente Medical Group, Woodland Hills, CA; Johns Hopkins Medical Institutions, Baltimore, MD.

Background: Neurofibroma (NF), a benign peripheral nerve sheath tumor, is very uncommon in the sinonasal tract, with only a few reported cases in the English literature.

Design: Cases within the files of the authors' institutions confined to the sinonasal tract were retrospective reviewed and compared to cases reported in the English literature (Medline 1966-2014).

Results: The 12 patients included 6 females and 6 males, aged 26-75 years (mean 46.2 years). The patients usually presented clinically with a mass lesion (n = 11), obstruction (n = 4) or pain (n = 3), with an average symptom duration of 42.9 months. Two patients had neurofibromatosis (NF1). Tumors involved the nasal cavity alone (n = 8), maxillary sinus alone (n = 2), or mixed sites (n = 2), with a range of 0.4-4.1 cm (mean 2.2 cm). The tumors were circumscribed, composed of bland spindled to wavy cells with curvilinear nuclei set in a background of collagenized stroma, mucopolysaccharide material and mast cells. Nuclear palisading and perivascular hyalinization were not seen. Mitoses were scant. Pleomorphism, necrosis and increased cellularity were absent. By immunohistochemistry, the lesional cells were positive with S100 protein (100%), SOX10 (58%) and NFP (75%), while the dendritic and perineurial-like cells were positive with CD34 (92%), calretinin (33%), and bcl-2 (92%). CD117 and calretinin highlighted mast cells. INI-1 was intact, with strong nuclear expression in all cases. All patients had surgical excision without recurrence (mean follow-up, 8.6 years). The principle differential diagnoses include schwannoma, perineurioma, fibromatosis, and solitary fibrous tumor.

Conclusions: NF of the sinonasal tract occurs in middle aged patients without a gender predilection, usually with non-specific symptoms present for a long duration. Tumors are relatively large (mean, 2.2), and usually affect one site only. Surgery is curative, with only 16.7% NF1 associated. S100 protein, SOX10 and NFP highlight the Schwann cells, with CD34 and bcl-2 highlight perineurial-like and dendritic cells.

1330 Aggressive Pattern of Invasion Predicts Occult Metastasis for Oral Cavity Cancer Patients

Claudia Velosa, Qiuying Shi, Simion Chiosea, William Carroll, Eben Rosenthal, Margaret Brandwein-Gensler. University of Alabama, Birmingham, AL; University of Pittsburgh Medical Center, Pittsburgh, PA.

Background: Patients with T1/T2 oral cavity squamous cell carcinomas (**OCSCC**) classified as cN0 face three options: elective neck dissection (**END**), elective adjuvant radiotherapy, or observation. Tumor depth of invasion (**DOI**) ≥ 4mm is one indication for ELD, as 15 - 20% of these patients will have pathologically positive cervical lymph nodes (**occult pN+**). Here we test the hypothesis that tumor worst pattern of invasion (**WPOI**) can predict clinically occult pN+.

Design: This cohort consists of 184 patients with T1/T2 cN0 OCSCC undergoing primary resection with END; patients with DOI < 4 mm were excluded. WPOI was classified as per the Risk Model (Head Neck Pathol, 7: 211-223, 2013). Outcome data were abstracted from the electronic medical records. Fisher's two-tailed exact test and Kaplan Meier outcome analyses were performed.

Results: Figure 1 presents Kaplan Meier curves for lymph node status, WPOI, and locoregional recurrence; both pN+ and WPOI-5 are significantly associated with fewer months to locoregional recurrence (truncated at 60 months). **Table 1** stratifies lymph node status (**pN0** versus **pN+**)by WPOI. Occult pN+ lymph nodes were found in **11.4%** (21/184) of patients, 13 patients were N1, 8 were N2. Ninety six percent of patients with either WPOI-3 or WPOI-4 were pN0; 4% of patients were occult pN+. In contrast only 64% of patients with WPOI-5 were pN0; 36% of patients were occult pN+. **WPOI- 5 is predictive of occult pN+, compared to WPOI-3/WPOI-4 (p < 0.0001).**

Figure 1. Time to Disease Progression and Lymph Node Status-WPOI

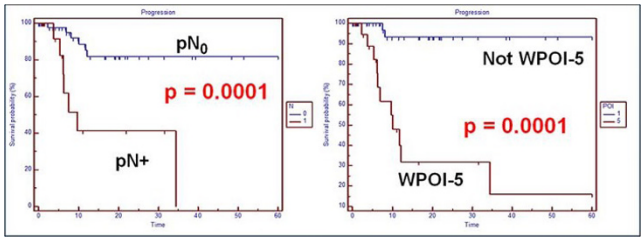

Table 1. Lymph Node Status by WPOI

pN	WPOI-3	WPOI-4	WPOI-5	Total
N0	57	77	29	163
N1	2	2	9	13
N2	0	1	7	8
	59	80	45	184

Conclusions: WPOI-5 is significantly predictive of the occult cervical metastases for patients with OCSCC and DOI ≥ 4mm. This can further refine the indications for performing END.

1331 A Limited Panel of Immunohistochemical Markers To Distinguish Basal Cell Carcinomas of Cutaneous Origin From Basaloid Squamous Cell Carcinoma of the Head and Neck

Gabriel Villada, Jennifer Chapman, Oleksandr Kryvenko, German Campuzano Zuluaga, Carmen Gomez-Fernandez. University of Miami Miller School of Medicine, Miami, FL; Jackson Memorial Hospital, Miami, FL.

Background: Cancer with basaloid features of the head & neck can be challenging to classify correctly. A classical problem is the distinction between a basaloid squamous cell carcinoma (bSCC) and a basal cell carcinoma (BCC) of cutaneous origin which may demonstrate squamous differentiation or a morpheaform pattern resembling bSCC. This is particularly true in small biopsies, and for patients who may present with metastasis and a remote history of skin cancer. A specific diagnosis is essential because of significant differences in clinical outcome and therapeutic management. Several immunohistochemical (IHC) markers have been described for differentiating these neoplasms. The aim of this study was to identify a limited optimal panel of IHC markers that may be used for this differential diagnosis.

Design: Ten cases each of bSCC and BCC resections of the head and neck diagnosed at our institution were selected based on primary location and the classic morphologic features that characterize these two entities. They were reviewed independently by two investigators to confirm the diagnosis. The following IHC stains were performed: CK14, BerEp4, EMA, p16, androgen receptor (AR), CD44, Bcl2 and CK8/18.

Results: The results are summarized in the following table:

IHC stains	bSCC(n=10)	BCC(n=10)	pvalue
CK14	7/10(70%)	10/10(100%)	0.210
BerEp4	5/10(50%)	10/10(100%)	0.032
EMA	10/10(100%)	0/10(0%)	
p16	8/10(80%)	0/10(0%)	
AR	4/10(40%)	9/10(90%)	0.057
CD44	10/10(100%)	5/10(50%)	0.032
Bcl2	4/10(40%)	6/10(60%)	0.656
CK8/18	9/10(90%)	5/10(50%)	0.141

There is a statistically significant difference between the staining patterns of bSCC and BCC for EMA, p16, BerEp4, and CD44. Although BerEp4 is considered to be a good IHC stain for carcinomas of cutaneous origin to differentiate BCC (usually positive) from SCC (usually negative), it is not useful in the differential of BCC vs. bSCC of the head & neck. p16 and EMA appear to be the more discriminative IHC markers.
Conclusions: bSCC and BCC of the head and neck can be readily distinguished by a limited panel consisting of EMA and p16. For those cases where p16 is negative, EMA is the optimal marker for this differential diagnosis.

1332 Receptor Tyrosine Kinases as Novel Therapeutic Targets in Head and Neck Squamous Cell Carcinoma

Anne von Massenhausen, Mario Deng, Wenzel Vogel, Andreas Schrock, Angela Queisser, Sven Perner. Institute of Pathology, University Hospital, Bonn, Germany; University Hospital of Bonn, Bonn, Germany.
Background: Malignant tumors of the head and neck region are the 6th most common malignancy world wide in which squamous cell carcinoma of the head and neck (HNSCC) are the most prevalent. However, next to surgery and radio and/or chemotherapy therapy options remain limited. Receptor tyrosine kinases (RTKs) offer suitable structures for targeted therapies that have fewer side effects than standard therapies. They bind growth factors, cytokines and hormones and regulate normal cellular processes as well as tumorigenesis. Small molecule inhibitors or antibodies for several RTKs are available. Since some RTKs are known to play a role in HNSCC we aimed to identify more RTKs that could be novel therapeutic targets for this tumor entity.
Design: Bioinformatic analysis of available data from The Cancer Genome Atlas (TCGA) was performed to identify RTKs that are frequently mutated in HNSCC (n=306). Subsequently immunohistochemistry (IHC) of these RTKs was done on a HNSCC cohort (n=336). HNSCC cells were transduced with lentiviral vectors containing FGFR3 or shRNA against AXL. Proliferation was assessed using MTT Assay.
Results: We identified 24 RTKs that are mutated in at least 2% of patients with HNSCC. Seven are already well described in head and neck cancer. Out of the remaining we performed IHC on our HNSCC cohort for RTKs for which small molecule inhibitors are available. AXL (AXL receptor tyrosine kinase), MERTK (c-mer proto-oncogene tyrosine kinase), FGFR3 (fibroblast growth factor receptor 3) and DDR2 (discoidin domain receptor tyrosine kinase 2) that are all mutated in 2% of cases showed positive IHC staining in 54.1%, 27.8%, 23.8% and 21.4% of primary tumors, respectively. ROS1 (c-ros oncogene 1, receptor tyrosine kinase), ALK (anaplastic lymphoma receptor tyrosine kinase) and RET (ret proto-oncogene) showed no expression in tumor tissue. HNSCC cells that overexpress FGFR3 showed increased proliferation and HNSCC cells with AXL knockdown proliferated less. AXL, MERTK and DDR2 will also be stably overexpressed in HNSCC cells. Subsequently, proliferation, migration/invasion as well as colony formation will be analysed upon treatment with and without small molecule inhibitors.
Conclusions: AXL, MERTK, FGFR3 and DDR2 are infrequently mutated but frequently overexpressed in HNSCC. Therefore we suggest that these RTKs could be novel therapeutic targets for this tumor entity.

1333 Druggable Genomic Landscape of Advanced Stage Non-Specialized Adenocarcinomas of Salivary Glands

Kai Wang, Timothy Jennings, Juliann Chmielecki, Siraj Ali, Julia Elvin, Roman Yelensky, Doron Lipson, Vincent Miller, Philip Stephens, Jeffrey Ross. Foundation Medicine Inc, Cambridge, MA; Albany Medical College, Albany, NY.
Background: Non-specialized adenocarcinomas of salivary glands (ACSG) include AC NOS and ductal AC and represent an aggressive subset of SG malignancies. We queried whether the genomic alterations in the ACSG group were different from those in specialized (differentiated) carcinomas of SG including mucoepidermoid, adenoid cystic and other specialized carcinomas (SCSG) and could lead to potential targeted therapy selection.
Design: DNA was extracted from 40 microns of FFPE sections from 92 clinically advanced ACSG and 110 SCSG (adenoid cystic, mucoepidermoid, mammary associated secretory, myepithelial, acinic cell and undifferentiated carcinomas). Comprehensive genomic profiling (NGS) was performed on hybridization-captured, adaptor ligation based libraries to a mean coverage depth of 682X for 3,230 exons of 182 cancer-related genes plus 37 introns from 14 genes frequently rearranged in cancer. The results were evaluated from a single sample for all classes of genomic alterations including point mutations, short insertions and deletion, amplifications and homozygous deletions and fusions/rearrangements.
Results: There were 30 (33%) female and 62 (67%) male patients with 2 grade 1, 27 grade 2 and 63 grade 3 ACSG. All ACSG were advanced stage at the time of comprehensive profiling with 27 Stage III and 65 Stage IV cases. There were 339 total alterations identified in SGCA group (3.7 GA per tumor). There were 178 clinically relevant alterations (1.9 per tumor) involving 49 different genes with 81 (88%) of ACSG featuring at least 1 actionable GA. The most frequent clinically relevant alterations included *PIK3CA* (25%); *HRAS* (20%); *CDKN2A* (17%); *ERBB2* (15%); and *PTEN*, *NF1*, *NOTHCH1*, *MCL1* and *EGFR* (range 5-9%). The greater frequency of *ERBB2* alterations in 14/92 (15%) in ACSG vs 1/110 (1%) of SCSG was significant (p=0.0001) as was a similar increase in *HRAS* alterations of 18/92 (20%) vs 4/110 (4%) (p=0.008).
Conclusions: ACSG are a clinically aggressive and pathologically distinctive subset of SG malignancies which differ significantly from the specialized SCSG tumors in their GA after comprehensive genomic profiling. The high frequency of clinically relevant alterations in ACSG including the 15% *ERBB2* alteration frequency suggests that continued molecular analysis of this tumor type has the potential to lead patients to clinical trials employing both established and novel targeted therapies.

1334 To Touch or To Hug? Introducing a Grading System for Perineural Invasion in Head and Neck Squamous Cell Carcinoma

Zhiqiang Wang, Sania Shuja, Jaime Morel, Carmela Monteiro, Raafat Makary. University of Florida College of Medicine, Jacksonville, FL; Emory University School of Medicine, Atlanta, GA.
Background: Perineural invasion (PNI) in head and neck squamous cell carcinoma (HNSCC) is known to be associated with local recurrence and regional lymph node metastasis, and is therefore a required data element in pathology reporting. However, there are no universally accepted diagnostic criteria for PNI. Consequently, in the literature there is a wide variation in the frequency of PNI reporting (from 2% to 82%). This study proposes a grading system for PNI that could be utilized for risk assessment and therapy in HNSCC.
Design: The grading system incorporates pattern and extent of PNI. "Touching pattern" denotes direct contact of tumor cells with the outer layer of perineurium. "Hugging pattern" is defined as tumor cells in contact with more than one-third circumference of the perineurium. Extent of PNI denotes whether PNI involves nerves within (intra-tumoral) or outside tumor (extra-tumoral). We hereby propose a 3-point grading system:
Grade 1: "Touching pattern", intra-tumoral PNI;
Grade 2: "Hugging pattern", intra-tumoral PNI;
Grade 3: "Touching" or "Hugging" pattern, extra-tumoral PNI.
Based on the proposed grading system, we reviewed 155 consecutive cases of HNSCC.
Results: Before applying the proposed criteria, there was unanimous consensus on PNI with the "Hugging pattern", but there was controversy with the "Touching pattern" among our group. After following the proposed criteria, a good consensus was reached for PNI with the "Touching pattern". Out of the 155 cases that were reviewed, PNI was noted in 62 cases (40%), with 34% grade 1, 53% grade 2, and 13% grade 3.
Conclusions: Our 3-point grading system is simple with clearly defined criteria and has the potential to improve accuracy and consistency in the diagnosis of PNI. The grading system may help in stratification of patients with high risk for local recurrence and regional lymph nodes metastasis. In addition, our proposed grading may provide added level of help to design treatment strategies and follow-up.

1335 Genotypic and Phenotypic Comparison of Polymorphous and Cribriform Adenocarcinomas of Salivary Gland

Ilan Weinreb, Simion Chiosea, Raja Seethala, Jorge Reis-Filho, Britta Weigelt, Salvatore Piscuoglio, Lei Zhang, Yun-Shao Sung, Manu Tirunagari, Cristina Antonescu, Alena Skalova, Lester Thompson, Bayardo Perez-Ordonez. University Health Network, Toronto, ON, Canada; University of Pittsburgh Medical Center, Pittsburgh, PA; Memorial Sloan Kettering Cancer Center, New York, NY; Charle's University, Plzen, Czech Republic; Woodland Hills Medical Center, Woodland Hills, CA, Canada.
Background: Polymorphous low-grade adenocarcinoma (PLGA) and cribriform adenocarcinoma of salivary gland (CASG) are low-grade tumors primarily arising in the oral cavity and oropharynx, respectively. PLGA is associated with a fascicular-targetoid pattern, while CASG has a glomerulopapillary pattern. Separation of these entities is controversial, particularly with respect to the distinctiveness of CASG. Recently an activating E710D hotspot mutation in *PRKD1* was found in 73% of PLGA. Rearrangement of *PRKD1-3* genes has been found in 75% of CASG and 50% of mixed cases. The morphology of these tumors has not previously been correlated with a complete molecular characterization.
Design: 52 cases with known molecular status were examined, blinded to molecular results. They were categorized as CASG (18), PLGA (17) or mixed (17). The latter group was subsequently divided according to whether CASG (6) or PLGA (11) was favored in an attempt to determine whether molecular status could be predicted by morphology.
Results: Of the 52 cases, 41 had rearrangement or mutation of a *PRKD* gene (79%). Of the 18 CASG cases, 15 (83%) showed fusion of a *PRKD* gene (8 *PRKD1*, 3 *PRKD2*, 4 *PRKD3*) and 2 showed *PRKD1* E710D mutation (11%). Of the 17 PLGA cases, 1 (6%) showed rearrangement of *PRKD2* and 7 showed *PRKD1* E710D mutation (41%). In the mixed category, there were 6 cases favored to represent CASG, with 5 (83%) showing rearrangement of a *PRKD* gene (2 *PRKD1*, 1 *PRKD2*, 2 *PRKD3*) and 1 showing a *PRKD1* E710D mutation (17%). In the 11 mixed cases favored to be PLGA there were 4 (36%) with a *PRKD* gene rearrangement (3 *PRKD1* and 1 *PRKD2*) and 8 cases with a *PRKD1* E710D mutation (73%). All remaining cases were negative for both. New morphologies associated with CASG/fusion status included canalicular, tall cell and microcystic features. Apocrine ducts, basaloid morphology and intracellular mucin were associated with PLGA and *PRKD1* E710D mutation. All pharyngeal cases were associated with rearrangement of a *PRKD* gene.
Conclusions: There is a clear genotype-phenotype correlation with fusion of *PRKD* genes associated with CASG morphology and pharyngeal site, and *PRKD1* E710D

hotspot mutation associated with PLGA morphology. However, overlap between the two groups exists on both a morphologic and molecular level. The fact that these two tumors are driven by genes in the same family also places them on a spectrum with one another.

1336 The Predominance of Apocrine Morphology and Androgen Receptor Positivity in 204 Cases of Salivary Duct Carcinoma

Lindsay Williams, Lester Thompson, Ilan Weinreb, Adel Assaad, Madalina Tuluc, Nasir Ud Din, Bibianna Purgina, Chi Lai, Christopher Griffith, Raja Seethala, Simion Chiosea. University of Pittsburgh Medical Center, Pittsburgh, PA; Southern California Permanente Medical Group, Woodland Hills, CA; University Health Network, Toronto, ON, Canada; Virginia Mason Medical Center, Seattle, WA; Thomas Jefferson University, Philadelphia, PA; Aga Khan University, Karachi, Pakistan; University of Ottawa, Ottawa, Canada.

Background: Salivary duct carcinoma (SDC) is a prototypic aggressive salivary gland carcinoma. Most SDCs are characterized by an apocrine phenotype (abundant eosinophilic cytoplasm, decapitation secretions, prominent nucleoli) and androgen receptor (AR) expression. Using terminology applied to breast carcinomas, such cases are categorized as 'luminal AR positive.' Our aim is to determine the prevalence of apocrine and other (e.g., basaloid, luminal AR negative) phenotypes in a large multi-institutional series of SDC.

Design: The morphologic spectrum of 204 SDCs was evaluated. AR status was determined by immunohistochemistry (IHC). Positivity was defined by an Allred score of 3 or greater. SDC with non-apocrine phenotype and AR negative were further studied by IHC (including p63, S100, estrogen receptor, HER-2/neu, mammaglobin, DOG-1) and fluorescence in situ hybridization (FISH) for *ETV6* or *MYB-NFIB*.

Results: 190 of 204 (93.1%) cases were of apocrine phenotype and the diagnosis of SDC was confirmed. AR IHC was technically adequate in 199 cases; 182 were AR positive and 17 were AR negative. 182 of 185 (98.4%) SDC were AR positive. Based on morphologic appearance and the results of additional studies, the 14 non-apocrine and AR negative cases were re-classified as:

epithelial–myoepithelial carcinoma with high grade transformation (HGT; n=2);
mammary analogue secretory carcinoma, high grade (*ETV6* translocated; n=1);
adenoid cystic carcinoma with HGT (*MYB-NFIB* intact; n=1);
acinic cell carcinoma with HGT (n=1);
myoepithelial carcinoma ex pleomorphic adenoma (n=1);
predominantly non-keratinizing squamous cell carcinoma (n=4);
adenosquamous carcinoma (n=1);
high grade adenocarcinoma, not otherwise specified (NOS; n=1);
carcinoma, NOS (n=2).

Conclusions: Non-apocrine AR negative SDC is extremely rare and the majority of such cases are more accurately classified as other entities altogether. Specifically, HGT of other salivary carcinomas and non-keratinizing squamous cell carcinoma are the most common mimics of SDC. If classification of breast carcinomas is extrapolated to SDC, it appears that practically all SDC fall into one category: 'luminal AR positive' SDC.

1337 Salivary Gland Basal Cell Adenocarcinomas and Basal Cell Adenomas: Similar Histology, Different Molecular Signature

Thomas Wilson, Deqin Ma, Anup Tilak, Robert Robinson. University of Iowa Hospitals and Clinics, Iowa City, IA.

Background: Basal cell adenocarcinoma (BCAC) and basal cell adenoma (BCA) represent uncommon basaloid salivary gland neoplasms that show morphologic and immunohistochemical similarity. While both are low grade, BCAC is locally aggressive and has the potential for distant metastasis. Controversy exists as to whether BCAC represents progression of BCA or is a separate process. Due to the low incidence of these tumors the molecular mechanism underlying their pathogenesis is poorly understood. We sought to further delineate these neoplasms through mutation profiling by targeted next-generation sequencing (NGS).

Design: Eight salivary gland BCAC and 9 BCA were retrospectively selected from our archives. NGS was performed using the Ion AmpliSeq™ Cancer Hotspot Panel v2 (Life Technologies, Carlsbad, CA). The data was analyzed using the Ion Torrent Suite Software (Life Technologies) followed by a laboratory developed/validated pipeline.

Results: Three of 8 cases of BCAC had mutations: one had a frameshift deletion in *ALK*, which is the first non-sense mutation identified in this gene; the second showed an activating mutation in *PIK3CA*, and the third had a non-pathogenic mutation in the *MET* gene. The *CTNNB1* I35T mutation, previously reported in BCA, was identified in 3/9 cases of BCA. A missense mutation in the *ATM* gene was seen in a different case with an allele frequency of 53%, raising the possibility of a germline mutation. A benign polymorphism of the *MET* gene was seen in another case. No mutations were detected in 5 cases of BCAC and 4 cases of BCA.

Tumor Type	Gene	Mutation Identified; Nucleotide, Amino Acid Change	Predicted Effect
BCAC	ALK	c.3605delG, p.G1202fs	Non-sense mutation
BCAC	PIK3CA	c.3140G>A, p.H1047R	Activating mutation
BCAC	MET	c.3029C>T, p.T1010I	Likely benign polymorphism
BCA	CTNNB1	c.104T>C, p.I35T	Affects degradation of beta-catenin
BCA	CTNNB1	c.104T>C, p.I35T	Affects degradation of beta-catenin
BCA	CTNNB1	c.104T>C, p.I35T	Affects degradation of beta-catenin
BCA	ATM	c.2572T>C, p.F858L	Inactivating mutation of tumor suppressor
BCA	MET	c.1124A>G p.N375S	Benign polymorphism

Conclusions: Activating mutations in oncogenes may be a mechanism for the development of BCAC while the Wnt signaling pathway may play a role in the pathogenesis of BCA. Aberrations in genes affecting different signaling pathways were seen in BCAC and BCA, suggesting that BCAC liekly arises de novo and not from BCA.

1338 A Novel Variant of EWSR1-ATF1 Fusion Gene in Hyalinizing Clear Cell Carcinoma

Hidetaka Yamamoto, Takafumi Nakano, Toshimitsu Nishijima, Yoshinao Oda. Kyushu University, Fukuoka, Japan.

Background: Hyalinizing clear cell carcinoma (HCCC) is a low-grade salivary gland carcinoma characterized by clear cells and hyalinized stroma. Recently, the EWSR1 gene rearrangement has been found in up to 80% of HCCCs by fluorescence in situ hybridization (FISH). In such cases, EWSR1 exon 11 is fused to ATF1 exon 3; however, only a few cases have been confirmed to have this type of fusion gene by reverse transcription polymerase chain reaction (RT-PCR).

Design: We examined EWSR1 gene rearrangement by FISH and EWSR1-ATF1 fusion gene by RT-PCR and direct sequencing in 4 cases of HCCC. The formalin-fixed paraffin-embedded (FFPE) specimens were used for these molecular analyses.

Results: The patients comprised two male and two females, ranging in age from 27 to 67 years. The tumors were located in the nasopharynx (n=2), root of tongue (n=1) and soft palate (n=1). Histologically, tumors were composed of nested or cord-like proliferations of epithelial cells with clear to pale eosinophilic cytoplasm, embedded in hyalinized and focally fibroedematous stroma. EWSR1 rearrangement was positive in 3/4 (75%) cases by FISH . Among the EWSR1 FISH-positive 3 cases, EWSR1 exon 11-ATF1 exon 3 fusion gene was positive in 2 cases and negative in 1 case by RT-PCR. Then, we investigated other possible break points of EWSR1 and ATF1, and found the fusion gene products involving EWSR1 exon 10 and ATF1 exon 5 in one case. Neither FISH nor RT-PCR was positive in the remaining 1 case.

Conclusions: We identified a novel variant of EWSR1-ATF1 fusion gene in HCCC. Recognition of variation of the fusion genes is helpful for the molecular diagnostic strategy of HCCC.

1339 Vascular Cell Adhesion Molecule-1 (VCAM-1) Expression and Tumor Infiltrating Lymphocytes (TILs) in Oral and Oropharnygeal Squamous Cell Carcinoma: A Pilot Onco-Immunological Study

Ming Zhang, Amy Ziober, Kathleen Montone. Hospital of the University of Pennsylvania, Philadelphia, PA.

Background: Human papillomavirus (HPV) infection is considered as an important etiology in the development of oropharyngeal and possibly some oral cavity squamous cell carcinomas (SCC). Only recently, immune responses in tumor microenvironment, mainly represented by tumor cells, mesenchymal stromal cells and tumor infiltrating lymphocytes (TILs), has been recognized to play a critical role in cancer progression and outcomes. Vascular cell adhesion molecule-1 (VCAM-1), an immunoglobulin–like adhesion molecule mainly expressed in endothelial, has been found to be expressed in various cancer. However, little is known about the expression and function of VCAM-1 in oropharyngeal and oral cavity SCC.

Design: Series of 24 cases of base of tongue (18) and oral tongue (6) SCC were subjected to study. The tumor differentiation, HPV status and pathological staging were collected. VCAM-1 immunoreactivity in tumor and stromal cells was evaluated semi-quantitatively as: negative; weak (1+): <30% cells with membranous staining; moderate (2+): 30%-60% cells with membranous staining; strong (3+):>60% cells with membranous staining. CD8+ TILs were also calculated (per high-power-filed).

Results: VCAM was not expressed in mature squamous epithelium; while weak and moderate staining was noted in benign basal cells and dysplastic squamous epithelium, respectively. Moderate or strong VCAM-1 expression was identified in all 24 invasive carcinomas. Neither p16 (HPV) status nor pathological staging was found to be statistically associated with VCAM-1 expression. The tumor-surrounding mesenchymal stromal cells, exhibited increased VCAM-1 expression (55% with 3+ and 38% with 2+) compared to the adjacent non-tumor infiltrating stromal cells (0% with 3+ and 8% with 2+). Interestingly, the strong (3+) stromal cell VCAM-1 expression was found to be associated with an advanced lymph node status (pN0: 0%, pN1:62.5%, and pN2:88.9%). Consistent with findings in other studies, HPV+ SCC is associated with significantly high CD8+ TILs compared to HPV- SCC (81.9/HPF vs 7.3/HPF, $p<0.001$).

Conclusions: Our pilot study indicates that VCAM-1 expression is markedly altered in both malignant squamous cells and tumor-surrounding mesenchymal stromal cells

in oropharyngeal and oral cavity SCC. The further investigation of tumor-stromal-TILs interactions may provide a new insight into the immune response in head and neck SCC progression and future strategy for target treatment.

Hematopathology

1340 Clinicopathologic and Next Generation Sequencing Analysis of Follicular Dendritic Cell Sarcomas

Anmaar Abdul-Nabi, Catherine Cottrell, Chad Storer, Friederike Kreisel, TuDung Nguyen. Washington University, St. Louis, MO.

Background: Follicular dendritic cell sarcoma (FDCS) is an uncommon malignancy characterized by a proliferation of spindled to ovoid cells with morphology and immunophenotype characteristic of follicular dendritic cells. Although the clinicopathologic features of these rare tumors have been extensively studied, specific gene mutations or chromosomal alterations associated with FDCSs are largely unknown.

Design: We retrospectively identified 11 FDCSs diagnosed at our institution between 2001 to 2014. The clinicopathologic features for these cases were collected from the clinical databases, along with treatment, overall survival, and follow-up data. 3 cases with available tissue underwent targeted next generation sequencing (NGS) analysis by a hybrid-capture approach to evaluate the coding region of 151 cancer-associated genes. Variants were called by VarScan 2.3.6, and following review, were categorized as clinically actionable, uncertain significance or benign, the latter used if they were polymorphic.

Results: The 11 FDCS cases presented at a median age of 51 years (range 28-71) with a 2.6 male: female ratio. The mean follow-up was 26.4 months (range 1-115). The sites involved at diagnosis included: liver, spleen, mediastinum, neck, lymph node, pharynx, rectum, and peritoneum. The tumors showed classic morphology of a FDCS, and all were CD21+ and/or CD35+. All but 2 cases did not recur/metastasize after treatment by surgery, radiation and/or chemotherapy. Targeted NGS revealed 2 to 6 novel non-synonymous coding (NSC) sequence variants per case predicted to modify protein function. Although the 3 cases shared no mutual NSC mutations, the impacted pathways/proteins included a receptor tyrosine kinase, PI3K signaling, and G-protein signaling. One case had a well-known PI3K pathway mutation documented in other cancers that is amenable to mTOR inhibitor therapy.

Conclusions: The FDCS in our cohort exhibited similar histopathologic and clinical features to that of other published series. The molecular landscape of these tumors varied, and the affected genes differed among the 3 cases. A targeted NGS approach for these rare tumors has clinical utility, revealing alterations in established signaling pathways, and identifying somatic mutations with known therapeutic implications. Future analysis of additional cases will help to determine common biological pathways which may be targets for new therapies.

1341 The Inhibitor of NF-κB Kinase, IKKβ, Regulates the Stability of the Hedgehog Transcription Factor GLI1

Nitin Agarwal, Chae Hwa Kim, Kranthi Kunkalla, Francisco Vega. University of Miami, Sylvester Cancer Center, Miami, FL.

Background: Constitutive activation of the Hedgehog (Hh) transcription factor, GLI1, has been demonstrated in many cancers including diffuse large B-cell lymphoma (DLBCL). Hh signaling provides survival signals to DLBCL cells. The mechanisms controlling GLI1 transcriptional activity are poorly characterized. Herein, we show that the inhibitor of NF-κB kinase, IKKβ, interacts, phosphorylates and stabilizes GLI1.

Design: To identify regulatory components that participate in the transcriptional activity of GLI1, we explored GLI1 putative interacting proteins by liquid chromatography tandem mass spectrometry following immunoprecipitation (IP) of endogenous GLI1. The binding between IKKβ and GLI1 was confirmed by IP assays. The role of IKKβ in blocking degradation of GLI1 was assessed by a set of experiments including transfection studies, pharmarcological inhibition and knocking down of *GLI1*. To identify IKKβ-dependent GLI1 phosphorylation sites, we co-transfected full length GLI1 and IKKβ constructs in 293T cells and the IKKβ-GLI1 complex was purified. Peptides resulting from digestion of GLI1 were analyzed by mass spectrometry. Mutational studies were also performed to assess the role of the identified IKKβ-mediated phosphorylated sites in GLI1 stability. These studies were performed on DLBCL cell lines (SUDHL4, DOHH2, OCI-Ly19, HBL-1) and 293T cells.

Results: GLI1 was found to be associated with full length IKKβ, but not with the kinase-dead IKKβ mutant (K44A). Short stimulation of DLBCL cells (SUDHL4 and DOHH2) with TNFα leads to GLI1 phosphorylation at Thr1074 and decreases binding between GLI1 and HECT-type E3 ubiquitin ligase, ITCH, resulting in decreased K48-linked GLI1 polyubiquitination and stabilization of GLI1 levels. We identified nine phosphorylation sites in the C-terminal region of GLI1. Point mutation of Thr 1074 to Ala prevents IKKβ-mediated GLI1 phosphorylation and facilitates GLI1-ITCH interaction, polyubiquitination and degradation of GLI1 in the proteasome. IKKβ stabilizes GLI1 but GLI1 was not requiered to activate canonical NF-kB pathway.

Conclusions: Our data links IKKβ-mediated NF-kB signaling to the transcriptional activity of GLI1 and illustrates a novel cross talk between these two pathways. This is of interest because activation of the NF-kB pathway is frequent in DLBCL and the connection between Hh and NF-kB pathways may open novel therapeutic avenues for DLBCL.

1342 B-Cell Lymphoma, Unclassifiable, With Features Intermediate Between Diffuse Large B-Cell Lymphoma and Classical Hodgkin Lymphoma – A Series of 24 Patients

Tariq Aladily, Sanam Loghavi, L Jeffery Medeiros, Roberto Miranda. University of Texas MD Anderson Cancer Center, Houtson, TX; University of Jordan, Amman, Jordan.

Background: B-cell lymphoma, unclassifiable, with features intermediate between diffuse large B-cell lymphoma (DLBCL) and classical Hodgkin lymphoma (CHL), also known as Gray zone lymphoma (GZL), is a rare disease that has been recently included in the WHO classification of tumors of hematopoietic and lymphoid tissues. Only few cases are available in the literature.

Design: We reviewed cases of GZL between 2000 and 2013 and extracted clinical and pathologic features.

Results: A total of 24 cases were identified. The median age at the time of diagnosis was 39 years (range 20-64). 13 patients were men and 11 were women (M:F 1.18). Mediastinum was the most common site: 18/24 (75%), followed by neck lymph nodes: 17/24 (71%). Clinical stage was as the following; stage II: 13/21 (62%), stage III: 5/21 (24%), stage IV: 3/21 (14%), while none had stage I disease. Histopathologically, four patterns were identified according to the morphologic and immunophenotypic profiles. Cases with the morphology of CHL but immunophenotype of DLBCL were the most common and attained better outcome than other subtypes. Complex cytogenetic aberrations were found in all tested cases. Chemotherapy (CT) was given to all patients, radiotherapy (RT) to 9/22 (41%) and stem cell transplant (SCT) to 6/22 (27%). The median event free survival was 9 months (range 0-54), while the median overall survival was 30 months (range 7-62). The rate of complete remission was 11/20 (52%), but relapse rate was common: 7/11 (64%), which occurred at a median interval of 15 months (range 5-24). Both regimens commonly used for the treatment of Hodgkin lymphoma and non-Hodgkin lymphoma attained similar results in our patients.

Conclusions: GZL represents a distinct type of lymphoma. Women were more commonly affected in this series. Treatment with standard regimens for CHL and DLBCL would obtain inferior results in GZL. Intensive CT, consolidation RT, SCT and targeted therapy would improve the outcome.

1343 Large Granular Lymphocytic Leukemia (LGL): A Detailed Clinicopathologic Analysis With Focus on STAT3 Expression Profile

Mustafa Al-Kawaaz, Marcello Gaudiano, Ghaith Abu-Zeinah, Jia Ruan, Attilio Orazi, Wayne Tam, Giorgio Inghirami, Julia Geyer. Weill Cornell Medical College, New York, NY.

Background: LGL is an indolent chronic lymphoproliferative disorder characterized by expansion of clonal T or NK cells. LGL is frequently associated with chronic immune stimulation. Transient oligoclonal and monoclonal populations are very common and are difficult to distinguish from true malignancy. Diagnostic criteria for LGL are controversial and are not well-defined. Recent studies have identified somatic STAT3 mutation in ~40% of LGL. It is unclear if the constitutive activation of the JAK/STAT3 pathway correlates with the presence of somatic mutation in LGL. The purpose of this study was to clinically validate use of STAT3 antibody in a cohort of well-defined LGLs.

Design: Thirty five patients diagnosed with LGL using strict WHO classification criteria and presence of monoclonal TCR gene rearrangement were selected. Immunohistochemical (IHC) staining for CD3, CD8, CD56, cMYC and pSTAT3 was performed. The region of exon 21 within the SH2 domain of STAT3 gene was interrogated by PCR-Sanger sequencing.

Results: There were 15 men and 19 women with mean age of 61 (27-84) years. Patients presented with anemia (22), neutropenia (16) and/or thrombocytopenia (12). Mean PB LGL count was 3.5 x 10^3/ul. Sixteen (47 %) patients had an associated viral infection or autoimmune disease. Nineteen (56 %) had a concomitant hematologic malignancy. Twelve (34%) patients required treatment. Positive IHC staining for pSTAT3 was seen in 6 (18 %) patients: 4 were previously healthy and 2 had another malignancy. pSTAT3 was negative in all patients with associated viral infection or autoimmune disease. IHC staining for cMYC was seen in 11 (32%) cases and positively correlated with pSTAT3 IHC. There was no statistical correlation between IHC pSTAT3/MYC status and patient's age, sex, cytopenia or need for therapy. No detectable oncogenic STAT3 (Y640F) mutations were identified.

Conclusions: LGL presents a diagnostic challenge due to lack of reliable markers. Contrary to previous reports, we did not detect proven oncogenic STAT3 mutations in a series of carefully selected, well-characterized cases of LGL. IHC pSTAT3 was seen in 6 (18%) cases. These patients may represent a unique group, since they had no documented associated inflammatory disorder. There was a trend for increased symptom severity with need for treatment in 50% (vs 32%) of these patients. Thus, in keeping with previous research, presence of IHC STAT3 in LGL may distinguish the subset of patients with true malignancy. Additional studies are in progress to define all somatic mutations within the JAK/STAT3-5 gene pathway.

1344 Utility of T-Cell Subset Flow Cytometric Analysis in the Diagnosis of Hodgkin Lymphoma

Ahmad Alkhasawneh, Ying Li, Christopher Carter. University of Florida, Gainesville, FL.

Background: Reference labs often perform flow cytometry without histology correlation. However, flow cytometry has a limited role in the diagnosis of certain lymphomas (e.g. Classic Hodgkin Lymphoma (CHL)), and histology correlation is necessary to exclude HL. Previous studies have reported increased CD4/CD8 double-positive T-cells by flow cytometry (FC) in Nodular Lymphocyte Predominant HL (NLPHL), but FC methods that reliably predict HL have not been demonstrated. In this study, we aim to demonstrate that FC can reproducibly predict the presence of HL in excisional lymphoid tissue through T-cell subset analysis.